Marine Chemistry 234 (2021) 103998

Contents lists available at ScienceDirect

Marine Chemistry

journal homepage: www.elsevier.com/locate/marchem

Determination of ambient dissolved metal ligand complexation parameters via kinetics and pseudo-voltammetry experiments

George W. Luther III [a,*], Katherine M. Mullaugh [b], Emily J. Hauser [a], Kevin J. Rader [c,1], Dominic M. Di Toro [c]

[a] School of Marine Science & Policy, University of Delaware, Lewes, DE 19958, USA
[b] Department of Chemistry & Biochemistry, College of Charleston, Charleston, SC 29424, USA
[c] Department of Civil and Environmental Engineering, University of Delaware, Newark, DE 19716, USA

ARTICLE INFO

Keywords:
Chemical speciation
Thermodynamics
Chemical kinetics
Metal-ligand complexes

ABSTRACT

Dissolved chemical speciation of metals in natural waters encompasses a wide range of inorganic and organic compounds including metal organic ligand complexes, ML. Because of the different filters used, "dissolved" speciation can range from simple metal-ligand complexes with an average size of about 0.66 nm (mass of <3 k-daltons) to nanoparticles of 1 to 100 nm to colloidal forms that are 10 to 200–400 nm in size. Strong metal-ligand, ML, complexes are normally considered to be in <1 nm size fraction. Over the last 3 decades, competitive ligand exchange – cathodic stripping voltammetry (CLE-CSV) titrations have been the method of choice to study complexation. These titrations primarily give information on the excess ligands in the sample rather than the actual ligand in $ML_{unknown}$ complexes because they require adding metal to the sample. Thus, metal-ligand CLE-CSV titrations do not provide much information on the actual ligand present in $ML_{unknown}$. However, pseudovoltammetry provides the thermodynamic stability constant, K_{therm}, for Zn, Cu, Cd and Pb as the $ML_{unknown}$ complex is destroyed by reduction at the Hg electrode to form metal(Hg). Pseudovoltammetry does not require the addition of any reagents to the sample, but cannot be performed for ions such as Fe(III) [and Mn(III)] because reduction of the ion results in the reduction of the metal ion in the complex without destroying $ML_{unknown}$. For these ions, kinetic experiments to recover the metal in the ML complex can provide information on the $ML_{unknown}$ dissociation rate constant, k_d, and the conditional equilibrium constant, $K_{condML'}$. In these kinetic experiments, a competitive ligand (L_{comp}) is added to the sample, and over time the ML_{comp} complex is measured by CSV. If all the metal in $ML_{unknown}$ is recovered, k_d of $ML_{unknown}$ can be determined. If only a portion of the metal in $ML_{unknown}$ is recovered, equilibrium is achieved and $K_{condML'}$ as well as k_d can be determined in a single experiment; k_f can then be calculated. We describe how these methods can be used to determine information on the actual $ML_{unknown}$ complex. We show that 7 thermodynamic, kinetic and speciation parameters (K_{therm}, $K_{condML'}$, $K_{condM'L'}$, k_f, k_d, $\alpha_{M'}$, $\alpha_{L'}$) for $ML_{unknown}$ complexes can be derived from a combination of two of these experiments. The approaches described here are useful to determine these parameters for known ML complexes once a ligand has been isolated by advanced separation methods (e.g., LC-MS) and reacted with a metal of interest.

1. Introduction

Understanding the strength of bonding in metal ligand complexes, ML, is one of the most important topics in marine chemistry and chemical oceanography because the uptake of metals as micronutrients (or toxins) is key to understanding phytoplankton productivity and CO_2 transformation to organic matter (e.g., Kim et al., 2015, 2016). The goal of this contribution is to review the methods that determine information on the thermodynamics and kinetics of metal ligand complexes (either known or unknown).

There are three principal ways that researchers report the value of a stability constant of a metal-ligand complex, ML. Two are conditional stability constants $K_{cond\ M'L'}$ (uncorrected for metal and ligand side reaction coefficients) and $K_{cond\ ML'}$ (corrected for the metal side reaction

* Corresponding author.
E-mail address: luther@udel.edu (G.W. Luther).
[1] Present address: Mutch Associates, LLC, 360 Darlington Avenue, Ramsey, NJ 07446

https://doi.org/10.1016/j.marchem.2021.103998
Received 15 January 2021; Received in revised form 5 May 2021; Accepted 26 May 2021
Available online 12 June 2021

coefficient only), and the third is the thermodynamic stability constant, K_{therm} (corrected for metal and ligand side reaction coefficients). In addition to the stability constants, it is equally important to understand the reactivity of a given ML complex, which is determined by kinetics experiments.

Because trace metals exist at (sub) nanomolar concentrations in seawater, electrochemistry has been the method of choice of experimentalists to determine metal speciation and complexation over the last 3 plus decades. Specifically, anodic stripping voltammetry (ASV) and competitive ligand exchange absorptive cathodic stripping voltammetry (CLE-adCSV or CLE-CSV) have been applied to determine the chemical speciation of metal ligand complexes as well as the total concentration of the metal in solution (normally after UV oxidation of the sample which decomposes organic compounds including ligands).

There are three main ways to use these voltammetric methods to determine information on the stability constant of a given metal ligand complex in the sample. The first approach that is most often used is the titration of the sample with metal [e.g., Fe(III), Cu(II)] followed by a CLE-adCSV measurement on each metal titration solution (e.g., Buck et al., 2012, 2016; van den Berg, 2006). The resulting titration curve is linearized to fit the titration data and to obtain the total ligand concentration [L] and the conditional stability constant, $K_{cond\ M'L'}$, of the metal unknown ligand complex, $ML_{unknown}$ (Omanović et al., 2015; Pižeta et al., 2015). This method provides information primarily on the excess ligand(s) in the sample as often the added competitive ligand is not able to outcompete the unknown ligand, $L_{unknown}$, bound to the metal because the equilibration time of the experiment is frequently not long enough. For field samples, the chemical structure of the ligand is unknown.

The second approach is to perform anodic stripping voltammetry on a sample by applying more negative potentials to break down the metal ligand complex to form the metal amalgam which can form for only the divalent cations of Cu, Zn, Cd, and Pb. This method is known as pseudovoltammetry as the resulting current is plotted versus each applied potential resulting in 's' shape waves indicative of the metal ligand complex that was destroyed. Because there are no additions of any chemical to the sample, this method gives direct information regarding the actual metal bound to an unknown ligand including the ligand concentration (related to the current observed) and the K_{therm}. The K_{therm} of the $ML_{unknown}$ complex is calculated from a comparison of its potential to the potentials of known ML_{known} complexes for which the thermodynamic stability constants, K_{therm}, are known. Here, potential versus log K_{therm} follows Nernstian behavior at the hanging mercury drop electrode (HMDE, Lewis et al., 1995a; Croot et al., 1999; Rozan et al., 2003; Tsang et al., 2006). For field samples, the chemical structure of the ligand is unknown, but the log K_{therm} comparison gives information about the ligand's character, which includes possible functional groups and the number of ligating atoms. More than one $ML_{unknown}$ complex can be detected in a single experiment.

The third approach can use either the ASV or CLE-CSV voltammetry methods to determine the kinetic parameters, which are then used to calculate the thermodynamic parameters, for ML complex formation (e.g., Wu and Luther III, 1995; Witter et al., 2000; Croot and Heller, 2012). These researchers showed that the values of $K_{cond\ M'L'}$ determined by kinetic analysis and metal addition were in excellent agreement with those from CLE-CSV metal titration experiments. The kinetic parameters are the rate constant for the formation of the complex, k_f, and the rate constant for the dissociation of the complex, k_d. The ratio of k_f/k_d gives the conditional stability constant, $K_{cond\ M'L'}$. The value of k_d for the actual metal ligand complex can be determined by adding a competitive ligand to the sample and following the recovery of the metal until it is completely recovered by the competitive ligand, L_{comp}, to form ML_{comp}. Normally, the value of k_f for the actual metal ligand complex cannot be readily determined unless the actual ligand can be isolated from the sample. This limitation can be addressed in three ways. First, the value of k_f can be estimated from the metal's rate of water exchange, which is an upper limit for k_f (Hudson et al., 1992; Luther III et al., 2015). For inorganic Fe', which includes hydroxide and other inorganic ligands bound to Fe(III), k_f in seawater is $8 \times 10^6\ M^{-1}\ s^{-1}$ (Hudson et al., 1992). Second, kinetics experiments to determine equilibrium behavior permit determination of $K_{cond\ ML'}$ (corrected for the metal side reaction coefficient) and k_d, from which k_f can be calculated. Third, with the development of better methods for compound separation followed by mass spectrometry (LC-MS) and NMR for structural elucidation, marine chemists now have the potential to do this evaluation after isolating the unknown ligand and then performing a kinetic experiment with the metal of interest. Obviously, there is a critical need to have methods to determine the thermodynamic, kinetic and speciation parameters for actual natural $ML_{unknown}$ complexes before and after separation and structural methods provide the ligand structure.

This paper begins by defining the terms for the physical chemistry of ML complexes (section 2). Then methods, with examples and calculations, are described to evaluate the 7 thermodynamic, kinetic and speciation parameters (K_{therm}, $K_{condML'}$, $K_{condM'L'}$, k_f, k_d, $\alpha_{M'}$, $\alpha_{L'}$) of ML complexes (sections 3–5). As the CLE-CSV method is the method most often used, it will not be discussed in detail, but is referred to as a point of comparison. Other kinetic and thermodynamic methods using electrochemical methods are discussed with the objective that they become a more important part of our arsenal when analyzing samples for ML complexation. Although emphasis is on electrochemical methods, other analytical techniques can be used to provide similar information (e.g., Luther III et al., 1999, 2015; Reid et al., 1993; Rose and Waite, 2003b).

2. Metal ligand stability constants

2.1. Conditional metal-ligand stability constants

Because the total metal concentration (c_M or $[M]_T$) is the parameter measured in natural waters by metal specific techniques (e.g., inductively coupled plasma mass spectroscopy, atomic absorption spectroscopy, voltammetry, ion selective electrodes), metal complexation is expressed as the conditional equilibrium constant, $K_{cond\ M'L'}$ (eq. 1), which is also equal to the ratio of the rate constant of complex formation, k_f, to the rate constant of complex dissociation, k_d.

$$K_{cond\ M'L'} = \frac{[ML]}{[M'][L']} = \frac{k_f}{k_d} \tag{1}$$

Here [ML] is the concentration of the metal ligand complex, and M′ and L′ are the concentrations of the metal and ligand that are not bound to each other. Although the metal can bind more than one organic ligand, we provide equations for a single ML complex for simplicity and for when a single ligand can be isolated by chromatography methods (LCMS, Bundy et al., 2018; Boiteau et al., 2019). **M′** is defined as all the inorganic forms of M (e.g., chloride, sulfate, carbonate, hydroxide, etc.), and **L′** is defined as all ligand forms that are bound to H^+, Mg^{2+}, Ca^{2+}, etc. These are related to the total metal $[M]_T$ and $[L]_T$ where eq. 2 shows $[M]_T$.

$$\begin{aligned} c_M = [M]_T = [M^{n+}] + [ML] + [MCl^+] + [MSO_4] + \ldots \text{ or} \\ c_M = [M]_T = [M^{n+}] + [ML] + \Sigma\,[MX]_i \end{aligned} \tag{2}$$

The free metal ion ($[M(H_2O)_6^{n+}]$), also abbreviated as $[M^{n+}]$ or $[M]_{free}$ to indicate its activity $\{M^{n+}\}$ plus the metal bound to only other inorganic ligands (chloride, sulfate, carbonate, hydroxide, etc.) equals [M′] as in eq. 3.

$$[M'] = [M]_T - [ML] = [M^{n+}] + [MCl^+] + [MSO_4] + \ldots \tag{3}$$

Eq. 3 can be expanded using the equilibrium expressions for each metal-inorganic ligand complex to give eqs. 4 and 5

$$[M'] = [M^{n+}]\left\{1 + K_{MCl}[Cl^-] + K_{MSO4}\left[SO_4^{2-}\right] + \ldots\right\} \tag{4}$$

$$[M'] = [M^{n+}] + [M^{n+}]\sum K_{MXi}[X]_i = [M^{n+}]\left(1 + \sum K_{MXi}\,[X]_i\right) \quad (5)$$

where the sum is for the free ligand concentration of all the inorganic ligands, X_i, in the solution. The fraction of a free metal, $\alpha_{M^{n+}}$, with respect to all inorganic interactions in solution *without considering the organic ligand* is given by eq. 6.

$$\alpha_{M^{n+}} = \frac{[M^{n+}]}{[M']} \quad (6)$$

On substitution of the equilibria for all inorganic forms of M (eq. 5) into eq. 6, $\alpha_{M^{n+}}$ is expanded into eq. 7.

$$\alpha_{M^{n+}} = \frac{1}{1 + \sum K_{MXi}\,[X]_i} \quad (7)$$

The reciprocal of eq. 7 is known as the inorganic side reaction coefficient for M′ (here given the symbol $\alpha_{M'}$ in eq. 8), which is frequently used in the literature.

$$\alpha_{M'} = \frac{[M']}{[M^{n+}]} = 1 + \sum K_{MXi}\,[X]_i \quad (8)$$

Substituting eq. 8 for M′ into eq. 1 leads to eq. 9.

$$K_{cond\ M'L'} = \frac{[ML]}{[M']\,[L']} = \frac{k_f}{k_d} = \frac{[ML]}{[M^{n+}]\alpha_{M'}\,[L']} \quad (9)$$

Expanding eq. 9 for the correction of all inorganic ligands gives a different conditional stability constant known as $K_{cond\ ML'}$, which is related to $K_{cond\ M'L'}$ by eq. 10.

$$(\alpha_{M'})\,K_{cond\ M'L'} = \frac{(\alpha_{M'})\,k_f}{k_d} = \frac{[ML]}{[M^{n+}]\,[L']} = K_{cond\ ML'} \quad (10)$$

These two stability constants are those normally reported in the environmental literature, so it is important that the reader be able to discriminate between them easily. Also, the values of the stability constants follow the order $K_{cond\ ML'} > K_{cond\ M'L'}$.

Rearranging eq. 10 gives eq. 10a in log format,

$$logK_{cond\ ML'} = logK_{cond\ M'L'} + log\alpha_{M'} = logk_f - logk_d + log\alpha_{M'} \quad (10a)$$

Similarly, if only the ligand side reaction coefficient information is known, eq. 10b is relevant. As $\alpha_{L'}$ is rarely known, $K_{cond\ M'\ L}$ is not reported in the literature.

$$logK_{cond\ M'L} = logK_{cond\ M'L'} + log\alpha_{L'} \quad (10b)$$

2.2. Thermodynamic metal-ligand stability constants for complexes of 1:1 stoichiometry

When the ligand is known as in laboratory experiments, similar corrections can be made for the free ligand concentration as its α_{Lj-} (and $\alpha_{L'}$) for complexes with H^+, Ca^{2+}, Mg^{2+}, etc. can be calculated. First, we describe the interactions of the ligand with H^+ only. This is useful when a ligand can be isolated and reacted later with a metal of interest in a medium other than seawater. Eqs. 2a and 5a (analogous to eqs. 2 and 5) describe the ligand interactions with only hydrogen ions and the metal of interest.

$$c_L = [L]_T = \left[L^{j-}\right] + [ML] + \left[HL^{1-j}\right] + \left[H_2L^{2-j}\right] + \ldots \quad (2a)$$

$$[L'] = [L]_T - [ML] = \left[L^{j-}\right] + \Sigma\,[HL]_n \quad (5a)$$

When the ligand and its *acid dissociation constants* are known, the general form for the fraction of the deprotonated ligand, $\alpha^{j-}_{H_n\ ligand}$, in solution without complexation to any metals including those natural to seawater (e.g., Mg^{2+}, Ca^{2+}) is used (eq. 6a, see Reid et al., 1993). The reciprocal of eq. 6a is the side reaction coefficient, $\alpha_{L'(H\ only)}$, eq. 8a. The right side of eq. 8a is from Ringbom and Still (1972) where β_n is the *cumulative protonation constant* and n is the number of bound hydrogen ions (H^+).

$$\alpha^{j-}_{H_n\ ligand} = \frac{K_1K_2\ldots K_j\,[H^+]^{n-j}}{[H^+]^n + K_1[H^+]^{n-1} + K_1K_2[H^+]^{n-2} + \ldots + K_1K_2\ldots K_j} = \frac{[L^{j-}]}{[L']} \quad (6a)$$

For NTA^{3-} and other triprotic anions (e.g., PO_4^{3-}), the expression for the fraction, $\alpha^{j-}_{H_n\ ligand}$, is:

$$\alpha^{3-}_{NTA} = \frac{K_1K_2K_3}{[H^+]^3 + K_1[H^+]^2 + K_1K_2[H^+] + K_1K_2K_3} = \frac{[NTA^{3-}]}{[NTA']}$$

$$\alpha_{L'(H\ only)} = \frac{1}{\alpha^{j-}_{H_n\ ligand}} = \frac{[L']}{[L^{j-}]} = 1 + \sum_{n=1}^{N}\beta_n\,[H^n] \quad (8a)$$

Second, when Mg^{2+}, Ca^{2+} and other cations (e.g., Sr^{2+}, Ba^{2+}) can bind the ligand, eqs. 2b and 5b are used to describe all ligand interactions in seawater. Now, eq. 8a expands to eq. 8b where α_{Lj-} is the fraction of the ligand and $\alpha_{L'}$ is the side reaction coefficient with respect to all interactions (H^+, Mg^{2+}, Ca^{2+}, etc.).

$$c_L = [L]_T = \left[L^{j-}\right] + [ML] + \left[HL^{1-j}\right] + \left[H_2L^{2-j}\right] + \ldots + \left[MgL^{2-j}\right] + \left[CaL^{2-j}\right] + \ldots \quad (2b)$$

$$L' = [L]_T - [ML] = \left[L^{j-}\right] + \Sigma\,[HL]_n + \Sigma\left[M^{2+}L\right]_i \quad (5b)$$

$$\alpha_{L'} = \frac{1}{\alpha_{Lj-}} = \frac{[L']}{[L^{j-}]} = 1 + \sum_{n=1}^{N}\beta_n\,[H^n] + \sum K_{(M^{2+})i\,L}\left[M^{2+}\right]_i \quad (8b)$$

Unfortunately, in natural waters, the ligand is normally unknown because there are several ligands that can bind the metal; thus, the conditional constant from eq. 1 can only be corrected for the free metal ion. A measure of the total ligand concentration can be determined by metal titration and other experiments [e.g., Bruland, 1989; Buck et al., 2012].

Expanding eq. 9 to include the free ligand with respect to all interactions in seawater (eq. 8b) leads to eq. 11. Thus, the activities, expressed as {}, of both the metal and ligand are known, and the thermodynamic constant can be calculated as in eqs. 11–13.

$$K_{therm} = \beta = \frac{[ML]}{[M']\alpha_{M^{n+}}\,[L']\alpha_{Lj-}} = \frac{[ML](\alpha_{M'})(\alpha_{L'})}{[M'][L']} = \frac{[ML]}{[M]_{free}\,\,[L]_{free}} \quad (11)$$

where $\alpha_{M^{n+}}\,[M'] = [M^{n+}]$ or M_{free}

$$K_{therm} = \beta = \frac{\{ML\}}{\{M^{n+}\}\,\{L^{n-}\}} = K_{cond\ M'L'}\,(\alpha_{M'})(\alpha_{L'}) = \frac{k_f}{k_d}(\alpha_{M'})(\alpha_{L'}) \quad (12)$$

In log format, eq. 12 becomes eq. 13 and 13a.

$$logK_{therm} = logK_{cond\ M'L'} + log\alpha_{M'} + log\alpha_{L'} = logk_f - logk_d + log\alpha_{M'} + log\alpha_{L'} \quad (13)$$

$$logK_{therm} = logK_{cond\ ML'} + log\alpha_{L'} = logk_f - logk_d + log\alpha_{M'} + log\alpha_{L'} \quad (13a)$$

Note that the values of these stability constants are in the order: $K_{therm} > K_{cond\ ML'} > K_{cond\ M'L'}$.

Eq. 13 shows the 7 possible ML parameters (K_{therm}, $K_{condML'}$, $K_{condM'L'}$, k_f, k_d, $\alpha_{M'}$, $\alpha_{L'}$) that provide information on both the ligand and metal in a ML complex. Experimentally, $K_{cond\ M'L'}$ is the parameter determined in metal titration experiments using either CLE-CSV or ASV. Unfortunately, this parameter gives information mainly on *excess* unknown ligand(s), xs $L_{unknown}$, in a sample as equilibration times are typically not long enough to remove the ligand from the metal (see section 5.3 for a Fe(III) example). The parameter $\alpha_{M'}$ is normally known or can be calculated (see Table 1 section 2.3), but the parameter $\alpha_{L'}$ is unknown. In sections 3–5, we describe how to measure several of these parameters. At least two experiments on a sample are needed to fully

Table 1
Relationship between the conditional stability constants ($K_{cond\ M'L'}$ and $K_{cond\ ML'}$) determined in UV irradiated seawater (pH ~8.0) and the *actual* thermodynamic stability constant (log K_{therm}) for several metals bound with EDTA and $Zn(NTA)_2^{4-}$. The log of $\alpha_{EDTA'}$ is 8.0. Data from Coale and Bruland (1988); Bruland (1989, 1992); Capodaglio et al. (1990) and Donat and Bruland (1990).

Complex	log $K_{cond\ M'L'}$	log $\alpha_{M'}$	log $K_{cond\ ML'}$	Calc. log K_{therm}	Lit. log K_{therm}
$ZnEDTA^{2-}$	7.9	0.32	8.22	16.22	16.3
$CuEDTA^{2-}$	8.6	1.38	9.98	17.98	17.94
$CdEDTA^{2-}$	7.7	1.55	9.25	17.25	16.5
$PbEDTA^{2-}$	8.6	1.54	10.14	18.14	18.0
$Zn(NTA)_2^{4-}$	6.09	0.32	6.41	–	14.03

describe these 7 parameters. For example, K_{therm} can be determined for Cu^{2+}, Zn^{2+}, Cd^{2+} and Pb^{2+} using pseudovoltammetry, and K_{therm} then be used to calculate $\alpha_{L'}$ from eq. 14 once kinetic experiments can be performed to determine k_d or $K_{condML'}$ (eq. 10a; see section 5.3).

$$logK_{therm} = \log K_{cond\ M'L'} + \log \alpha_{M'} + \log \alpha_{L'} = logK_{cond\ ML'} + \log \alpha_{L'} \quad (14)$$

2.3. Literature data regarding the relationship of the parameters in eq. 12

K_{therm} is a pH and solution species independent constant as all solution conditions are properly specified. However, in environmental samples, the interactions of H^+, Ca^{2+}, and Mg^{2+} with the ligand are almost always unknown, so only conditional stability ML constants ($K_{cond\ ML'}$ or $K_{cond\ M'L'}$) are reported. Table 1 shows the conditional constants, $K_{cond\ M'L'}$ for $[M(EDTA]^{2-}$ complexes of +2 cations determined in seawater by anodic stripping voltammetry metal titration techniques (Coale and Bruland, 1988; Bruland, 1989, 1992; Capodaglio et al., 1990) as well as their known thermodynamic constants. $Zn(NTA)_2^{4-}$ data (Donat and Bruland, 1990) are also given in Table 1.

2.4. Thermodynamic metal-ligand stability constants for complexes with stoichiometry different from 1:1

For a complex with more than one ligand bound to a metal to form ML_y, eq. 11 is expressed as eq. 15 (eq. 15a, log format).

$$K_{therm} = \beta = \frac{\{ML_y\}}{\{M^{n+}\}\{L^{j-}\}^y} = K_{cond\ M'L'}\ (\alpha_{M'})(\alpha_{L'})^y \quad (15)$$

$$\begin{aligned} logK_{therm} &= logK_{cond\ M'L'} + log\alpha_{M'} + y\log\alpha_{L'} \\ &= logk_f - logk_d + log\alpha_{M'} + y\log\alpha_{L'} \end{aligned} \quad (15a)$$

For example y equals 2 for $[Zn(NTA)_2]^{4-}$. This equation can be expanded for mixed organic ligand complexes, ML_1L_2, that are reported in the inorganic chemistry literature (e.g., Fe(III) complexes in Taylor et al., 1994) where L_1 and L_2 are different organic ligands.

For a complex with more than one metal bound to more than one ligand combining to form a multinuclear metal cluster (M_xL_y), eq. 11 is expressed as eq. 16.

$$K_{therm} = \beta = \frac{\{M_xL_y\}}{\{M^{n+}\}^x\{L^{j-}\}^y} = K_{cond\ M'L'}\ (\alpha_{M'})^x(\alpha_{L'})^y \quad (16)$$

$$logK_{therm} = logK_{cond\ M'L'} + x\log\alpha_{M'} + y\log\alpha_{L'} \quad (16a)$$

$$logK_{therm} = logk_f - logk_d + x\log\alpha_{M'} + y\log\alpha_{L'} \quad (16b)$$

For the anionic cluster $[Zn_4S_6]^{4-}$ (Luther III et al., 1999), x equals 4 and y equals 6.

The K_{therm} equations above take into account pH as hydroxide and oxide ligand complexes are species in M′ that vary with pH according to hydrolysis constants, e.g., for MOH, etc. We note that some researchers (e.g., Kim et al., 2016; Lewis et al., 1995a, 1995b; Luther III et al., 1999; Taylor et al., 1994) have titrated complexes or changed the pH to determine if there is a change in the ML complex on acidification. Lewis et al. (1995a, 1995b) noted that catecholate binding shifted to weaker salicylate binding as K_{therm} decreased by six orders of magnitude for the ligand alterobactin-B when the pH was changed from 8 to 6; in this case, the side reaction coefficients for both the metal and ligand decrease.

K_{therm} values at 25 °C and corrected for seawater ionic strength for known ML complexes used in this work (Tables 2, 4 and Appendix Tables 5-7) are taken from the compilations of Martell and Smith (1974, 1977, 1982, 1986) unless otherwise specified.

2.5. Literature data regarding the metal ion side reaction coefficient, $\alpha_{M'}$

The speciation of Fe with organic ligands has generated immense interest since the first reports of FeL complexes in the water column of the ocean (Rue and Bruland, 1995; van den Berg, 1995; Wu and Luther III, 1995). Table 2 shows the conditional and thermodynamic constants for several natural or known ligands, L_{known}, bound to Fe(III) in seawater determined by our group; similar data have been obtained by González et al. (2019) for phenols including catecholates. Note that the side reaction coefficient for Fe' in seawater (log $\alpha_{Fe'} = 10$) is over eight orders of magnitude larger than that for the divalent cations in Table 1 because of Fe(III) hydrolysis to form hydroxo species. Thus, these $K_{cond\ ML'}$ constants are several orders of magnitude higher than those for the Group II cations in Table 1. See Table 3 for more log $\alpha_{M'}$ values of metals.

2.6. Literature data regarding the ligand side reaction coefficient, $\alpha_{L'}$

The evaluation of the ligand side reaction coefficient, $\alpha_{L'}$, is the major missing component to our understanding of $ML_{unknown}$ complexes. Table 3 provides some information from several sources on log $\alpha_{L'}$ for known ligands, which have been used to calibrate the three

Table 2
Relationship between the conditional stability constants and the thermodynamic stability constant for Fe(III)-complexes bound to several natural ligands in seawater modified from Witter et al. (2000). The log of $\alpha_{Fe'}$ in seawater at pH = 8 and a temperature of 20 °C equals 10.0 (Hudson et al., 1992). Appendix Figs. 9–11 give the structures for ligands in this work.

Complex	log k_f	log k_d	log $K_{cond\ M'L'}$	log $K_{cond\ ML'}$	log K_{therm}
Fe-ferrichrome (hydroxamate)	5.56	−7.30	12.9	22.9	29.1
Fe-desferrioxamine-B (hydroxamate)	6.29	−5.82	12.1	22.1	31.0
Fe-alterobactin-A	5.58	−6.76	12.3	22.3	51
Fe-protoporphyrin-IX	5.79	−6.15	11.9	21.9	–

Table 3
Some metal and ligand side reaction coefficients in seawater (pH ~ 8).

Metal ion	log $\alpha_{M'}$[a]	Ligand, ML stoichiometry	log $\alpha_{L'}$
Zn^{2+}	0.32	EDTA, FeL[b]	8
Cu^{2+}	1.38	NTA, FeL_2 2 $\log_{\alpha NTA} = 7.62$[c]	3.81
Cd^{c}	1.55		
Pb^{c}	1.54		
Ag^{c}	5.22	ferrichrome (tris-hydroxamate), FeL[d]	6.2
Mn^{d}	0.23	desferrioxamine-B (tris-hydroxamate), FeL[d]	8.9
Fe^{d}	0.16	desferrioxamine-B (tris-hydroxamate), FeL[e]	6.25
Co^{2+}	0.35		
Ni^{2+}	0.33	alterobactin-A [(bis-β-hydroxyaspartate)catecholate], FeL[d]	28.7
Cu^{+}	1.38		
Al^{3+}	8.88	alterobactin-B (bis-catecholate), FeL_2 2 $\log_{\alpha AltB} = 21.1$[d]	10.55
Cr^{3+}	5.59	enterobactin (tris-catecholate), FeL[f]	28.2
Fe^{3+}	10		

[a] Al-Farawati and van den Berg (1999).
[b] Coale and Bruland (1988).
[c] Donat and Bruland (1990).
[d] Witter et al. (2000) and van den Berg (2006).
[e] Schijf and Burns (2016) and Wuttig et al. (2013).
[f] Wu and Luther III (1995).

voltammetric methods or approaches noted in the introduction (the CLE-CSV titration, pseudovoltammetry and kinetic approaches). For comparison purposes, the values for log $\alpha_{M'}$ of several metals are also provided (data from Byrne et al., 1988; Al-Farawati and van den Berg, 1999).

The log $\alpha_{L'}$ for EDTA is from Coale and Bruland (1988). For NTA, Donat and Bruland (1990) calculated a value of log $\alpha_{L'}$ 7.62 from the data in Table 1 while assuming a 1:1 complex for $ZnNTA^{-}$. However, the 1:2 complex for $Zn(NTA)_2^{4-}$ is the dominant form (Lewis et al., 1995a); thus, the value for log $\alpha_{L'}$ NTA is 3.81 (from eq. 16a).

$$logK_{therm} = logK_{cond\ M'L'} + log\alpha_{M'} + 2log\alpha_{NTA'} \quad (16a)$$

$$logK_{therm} = 14.03 = 6.06 + 0.32 + 2log\alpha_{NTA'}$$

$$7.62 = 2log\alpha_{NTA'}$$

Schijf and Burns (2016) estimated a log $\alpha_{DFO\text{-}B'}$ of 6.25 for desferrioxamine-B (DFO-B) from its acid dissociation constants and its stability constants with various seawater cations. Wuttig et al. (2013) calculated a similar value. The other values of log $\alpha_{L'}$ in Table 3 are calculated from k_d, k_f and K_{therm} data found in Witter et al. (2000) using eq. 13 as will be shown in section 5.3. Interestingly, Witter et al. (2000) and van den Berg (2006) estimated the value of log $\alpha_{DFO\text{-}B'}$ in seawater to be 8.9 and 9.0, respectively. For enterobactin, Wu and Luther III (1995) calculated log $\alpha_{enterobactin'}$ from eq. 14 after evaluating $K_{condML'}$ (section 5.3) and knowing K_{therm} from Loomis and Raymond (1991). Table 3 data suggest that the log $\alpha_{L'}$ for each catecholate group binding to Fe(III) is ~9 and each hydroxamate group is ~2–3.

3. Pseudovoltammetry/Pseudopolarography: determination of K_{therm} for an actual (natural) ML in a sample

3.1. General procedure

Using a hanging mercury drop electrode (HMDE), the method of pseudovoltammetry has been used to study the metals Cu^{2+} (Croot et al., 1999), Zn^{2+} (Lewis et al., 1995a), Cd^{2+} (Tsang et al., 2006) and Pb^{2+} (Rozan et al., 2003) in seawater at natural levels with a variety of organic ligands. As shown below, these studies show Nernstian electrode behavior. Branica and Lovrić (1997) and others have used this approach to study single ML complexes. The theory for modeling individual pseudopolarogram waves has been provided by Omanović and Branica (2004) for hanging mercury drop electrodes (HMDE) and for thin mercury film electrodes by Lovrić (1998).

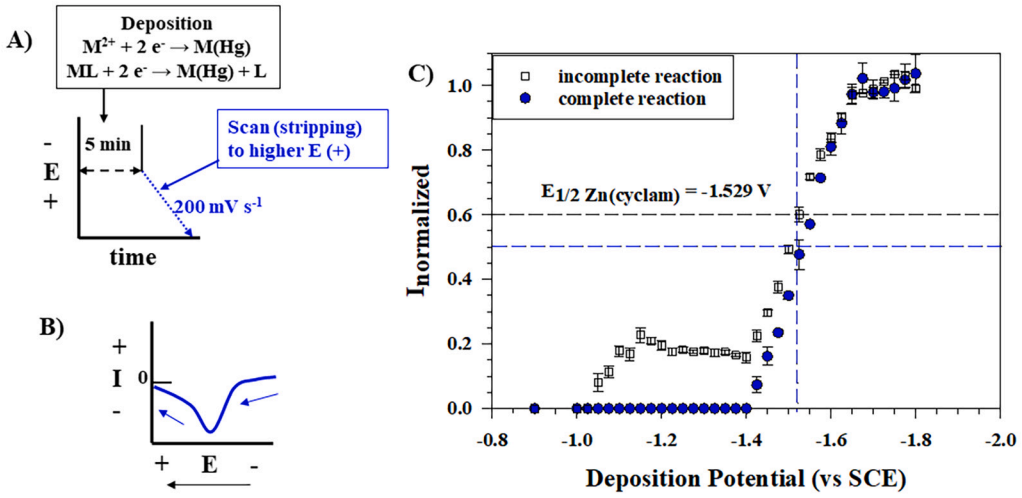

Fig. 1. A) The deposition potential is applied for the time desired, followed by a DC voltage scan to strip the metal from the Hg. B) The peak height from the scan gives the current and concentration of the metal stripped from the Hg electrode. C) Pseudovoltammograms of Zn^{2+} with cyclam in 10-fold excess in UV irradiated seawater (mean of triplicate experiments).

Pseudovoltammograms (*I* vs E_{dep} plots) are generated on less than 10 mL of sample using −0.020 to −0.050 V incremental deposition potentials over a potential range from −0.05 to −1.70 V (vs SCE) depending on the metal; thus, there is no need to add any reagents to a sample. *The range must include potentials before and after the reduction of the 'free' metal.* The 'free' metal is identified by its specific metal reduction potential [e.g.; −0.20 V (Cu^{2+}); −0.43 V (Pb^{2+}); −0.56 V (Cd^{2+}) and − 1.08 V (Zn^{2+})] in natural waters. (Sub)nanomolar detection limits can be achieved by using 30-min depositions, but this increases the duration of the experiment. After each deposition potential is applied (Fig. 1A) over the desired range, an anodic stripping experiment is performed using for example linear sweep voltammetry (LSV; scan rate 2000 mV s^{-1}) or square wave voltammetry (SWV; 100 mV s^{-1} scan rate; 20 mV pulse height) from the deposition potential to a final potential of −0.05 V. The peak current determined (Fig. 1B) is for the free metal ion that is stripped off the electrode as the complex cannot reform during the positive scan due to slow reformation kinetics at the electrode surface. The peak current (or the concentration) is plotted versus the deposition potential (*I* vs E_{dep}; Fig. 1C). At potentials more positive of the M^{2+} or ML reduction potential, the current will be '0'. As E_{dep} becomes more negative, the 'free' metal and any ML complex, if present, will be reduced to the M(Hg) and give a current during the anodic stripping experiment. One or more 's' shaped waves may be produced and the $E_{½, ML}$ of the ML complex occurs where the current, I, is at the half height of the 's' wave. In Fig. 1C, the square symbols show an incomplete reaction of Zn^{2+} with cyclam in seawater, and the half height is at 0.6 (black dashed horizontal line) as the initial normalized current increase of 0.2 is due to 'free' or inorganic Zn(II). The blue circles show the half height at 0.5 for complete formation of $Zn(cyclam)^{2+}$ (blue dashed horizontal line) after reacting overnight. The vertical dashed line indicates the $E_{½, ML}$ for $Zn(cyclam)^{2+}$. Fig. 1C demonstrates that the rate constant, k_f, for formation of ML complexes (see section 5.4) can be determined by performing several pseudovoltammetry experiments over time.

3.2. Theory of electrode processes to develop the 'chelate scale'

For metal ions (Cu^{2+}, Zn^{2+}, Cd^{2+} and Pb^{2+}) that can be reduced at the Mercury electrode to form the metal amalgam, M(Hg), many ML complexes can be broken down at the electrode as per eq. 17.

$$ML + 2\,e^- \rightarrow M(Hg) + L^{2-} \text{ (overall electrode reaction)} \quad (17)$$

The voltage, *E*, is a measure of the voltage needed to *destroy the ML complex to form M(Hg)* at the electrode and is related to the Gibbs free energy and the thermodynamic stability constant, K_{therm}, via eq. 18.

$$\Delta G = -nFE = -(RT)\,ln\,K_{therm} = \Delta H - T\Delta S \quad (18)$$

Eq. 17 is irreversible as the ML complex does not reform at the electrode when performing cyclic voltammetry experiments (Lewis et al., 1995a); only the 'free' metal gives a current signal on the reverse scan as it is 'stripped' off the Hg.

Although the electron transfer at the Hg electrode is inner sphere for inert complexes as the metal ion must be in contact with the electrode, eq. 17 can be modeled as two eqs. 19 and 20.

$$ML \leftrightarrow M^{2+} + L^{2-} \text{ (dissociation/destruction of the ML complex)} \quad (19)$$

$$M^{2+} + 2\,e^- \rightarrow M(Hg) \text{ (reduction of the metal ion)} \quad (20)$$

Thus, *E* is related to K_{therm} via the Nernst eq. (21)

$$E_{½,ML} = E_{½,\,M\ inorganic} - \frac{2.303\,RT}{\alpha nF}\,log\,K_{therm} \quad (21)$$

where $E_{1/2,\ M\ inorganic}$ is the reduction potential of the oxidized metal water complex, $M(H_2O)_6^{2+}$, plus any weak or labile complexes with inorganic anions. $E_{1/2,\ ML}$ is the reduction potential of the metal ligand, ML, complex. *F* is the Faraday constant, *R* is the ideal gas constant, T is the temperature in Kelvin, α is the kinetic transfer coefficient and is discussed below, and *n* is the number of electrons transferred at the electrode.

Eq. 21 is a form of the Lingane equation and assumes:

(a) $E_{½,\ ML}$ has no dependence on the reduced metal complex since the metal is reduced to an amalgam and the complex is destroyed, which is a measure of the bond strength and K_{therm}. Lewis et al. (1995a) noted that the value of $E_{½,\ ML}$ is similar at nM (deposition experiments) and μM concentrations (fast scans with no deposition) of metal and ligand.

(b) A strong and inert ML complex (defined as log $K_{therm} \geq 6$) acts as a discrete species and does not dissociate at the electrode prior to electron transfer, but its wave (peak) exhibits Nernstian behavior and its potential is independent of the concentration of L. [Strong $ML_{unknown}$ complexes in seawater are considered inert (e.g., Buck et al., 2012; Buck et al., 2016).] A weak ML complex (defined as log $K_{therm} \leq 6$) also gives a wave (peak), but can dissociate at the electrode; the peak potential will depend on the concentration of L (DeFord and Hume, 1951; Luther III et al., 2000). Information from strong and weak ZnL complexes are described below.

A plot of $E_{½,\ ML}$ versus $log\,K_{therm}$ for a series of ligands bound to the same metal is called a 'chelate scale' and can be constructed from literature K_{therm} constants (e.g., Fig. 2). $E_{½,\ ML}$ is measured in the matrix of interest; e.g., seawater. Thermodynamic constants for unknown ML complexes can then

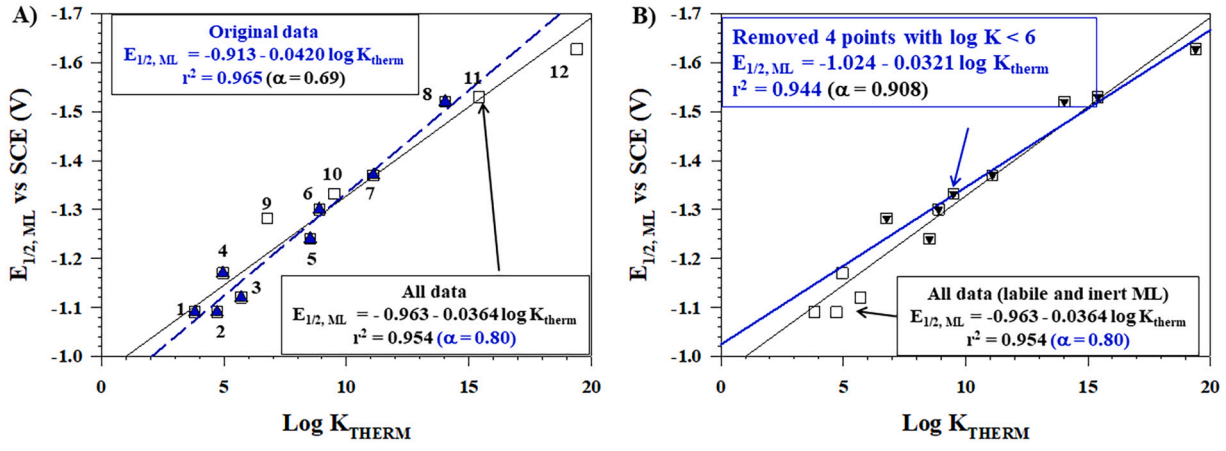

Fig. 2. A) Data for ZnL chelate scale (triangles) from Lewis et al. (1995a) and with additional data (squares, this work). B) Comparison of data for inert and labile ZnL complexes (squares) and only inert complexes (triangles).

Table 4
Data and information for various organic ligands bound to Zn^{2+}. $E_{1/2,\ ML}$ data obtained in seawater at pH = 8.

Ligand, data # for Fig. 2	stoichiometry	log K_{therm}	$E_{1/2,\ ML}$
UV seawater			−1.090
Oxalic acid - 1	ZnL	3.81	−1.090
CTP – 2	ZnL	4.72	−1.090
Glycine – 4	ZnL	4.96	−1.170
Ethylenediamine - 3	ZnL	5.7	−1.120
Iminodiacetic acid (IDA)[a] - 9	ZnL	6.77	−1.282
8-Hydroxquinoline – 5	ZnL	8.52	−1.240
IminoBis(MethylenePhosphonic Acid)IBMPA –6	ZnL	8.89	−1.300
Penicillamine[a] - 10	ZnL	9.50	−1.332
EDDA – 7	ZnL	11.1	−1.370
NTA – 8	ZnL_2	14.03	−1.520
EDTA	ZnL	16.30	ND
CDTA	ZnL	19.21	ND
Cyclam[a] - 11	ZnL	15.40	−1.529
Penicillamine[a] - 12	ZnL_2	19.40	−1.627

[a] Indicates our recently obtained data for complexes not published in Lewis et al. (1995a). ND indicates no signal due to electron transfer kinetic effects. Ligand structures for Zn complexes are given in Appendix Fig. 9. K_{therm} data from Martell and Smith (1974, 1977, 1982, 1986); $T = 25$ °C and corrected for the ionic strength of seawater.

be estimated by measuring the $E_{½,\ ML}$ of the $ML_{unknown}$ complex. Ionic strength corrections for the thermodynamic constants of known ML complexes may be necessary when using literature data because the value of $E_{½,\ ML}$ may vary slightly with the matrix chosen.

If the value of the slope, (2.303)RT/(nF), for a chelate scale deviates from Nernstian behavior (for $n = 2$, the slope should be 0.0296 V), then a kinetic effect occurs. The kinetic effect is described by α, the transfer coefficient, denoting the fraction of the potential influencing the rate of electro-reduction. Alpha values range as $0 < \alpha < 1$; the higher the α value, the smaller the kinetic effect. Using a vibrating gold or silver amalgam electrode, two other groups have performed pseudovoltammetry experiments on Cu^{2+} (Gibbon-Walsh et al., 2012) and Pb^{2+} (Bi et al., 2013), respectively. These studies were designed to enhance detection limits. Although the results did not show the expected Nernstian slope found at the HMDE, a linear chelate scale was determined. The slope for the Pb^{2+} study was 0.0560 V, and for the Cu^{2+} study 0.090 V.

To illustrate the assumptions used in eq. 21, Fig. 2 shows chelate scales for known ZnL complexes. Fig. 2A shows the original 8 data points from Lewis et al. (1995a) plotted as upward triangles. The slope for the Nernst eq. 21 is 0.420 V with an α value of 0.69. Four of the 8 ML complexes are labile and have a value of log $K_{therm} < 6$. Since that paper, we have determined $E_{½,\ ML}$ for 4 more inert ZnL complexes (see Table 4). Fig. 2A shows that the inclusion of all data for the twelve ZnL complexes (squares) now gives a Nernst slope of 0.0364 V. Fig. 2B replots all the data in Fig. 2A, but also gives a regression for only inert ZnL complexes (downward triangles). The Nernst slope is now 0.0321 V with an α value of 0.91, which documents that eq. 21 is most reliable for inert ML complexes. Based on the K_{cond} data obtained from environmental samples using metal titration experiments, strong inert $ML_{unknown}$ complexes are expected. The linear regressions for all plots show that the data follow Nernstian behavior, but it is advisable to use data for only inert ML complexes to generate a chelate scale.

Figs. 3A-C are composed from the data in the Appendix Tables 5-7 and show similar Nernstian behavior for various ligands with Cu^{2+} (Croot et al., 1999), Pb^{2+} (Rozan et al., 2003) and Cd^{2+} (Tsang et al., 2006) in seawater, respectively. The linear regressions for these plots also show that the data follow Nernstian behavior according to eq. 21. Cd^{2+}, Zn^{2+} and Pb^{2+} show the smallest kinetic effect (highest α values) as these are soft metals (Pearson, 1988) that form amalgams easily. The Cd^{2+} and Pb^{2+} chelate scales were performed with inert complexes and only one labile ML complex; regressions of the scales with and without the one labile ligand are not statistically different. The values for the intercepts in these equations indicate the approximate potential for the reduction of the metal ion in seawater, which includes the metal bound to labile inorganic ions (e.g., water, chloride, sulfate, carbonate, hydroxide, etc.).

3.3. Information from chelate scales

All chelate scales are from soft metals and show that log K_{therm} increases as the number of ligating atoms per molecule increases (increased denticity; Luther, 2016); e.g., for a 1:1 complex, $M(EDTA)^{2-} > M(NTA)^{-} > M(oxalate)$. EDTA binds with 6 atoms, NTA with 3 or 4 atoms and oxalate with 2 atoms. Log K_{therm} also increases as N and S atoms replace O atoms as the ligating atoms; e.g., the bidentate complexes follow the order M(pencillamine; N,S atoms) > M(glycine, N,O atoms) > M(oxalate, 2 O atoms). For Zn^{2+}, a reduction potential for the EDTA and CDTA complexes could not be obtained as Zn^{2+} is small (88 pm) and has a maximum of 6 coordination. Thus, an inner sphere electron transfer from the electrode to the Zn^{2+} cannot occur. Cu^{2+} exhibits Jahn Teller distortion so can easily contact the electrode surface to be reduced even though its size is 87 pm. Cd^{2+} (109 pm) and Pb^{2+} (133 pm) can expand coordination numbers to larger than 6 allowing for easier reduction of the M^{2+} in the ML complex at the electrode surface. These data give a rationale for the lack of a reduction wave for the Zn^{2+} complexes of EDTA and CDTA, and indicate these complexes are inert to ligand dissociation.

At a HMDE, pseudovoltammetry experiments can be performed to about −1.7 or − 1.8 V versus SCE as Na^{+} reduction can interfere beyond that; if a sample is acidified, the reduction of H^{+} will occur at more positive potentials and can also interfere. Thus, the highest K_{therm} values that can be determined are related to being able to discriminate the 's' shaped ML reduction peak from Na^{+} reduction interference. As deposition experiments are performed every 20 to 25 mV, the most negative $E_{1/2,\ ML}$ that can be determined is about −1.627 V [see Table 1 for Zn $(pencillamine)_2$]. Using the equations in Figs. 3A-D, the highest value for log K_{therm} that can be evaluated is near 19.8 for Zn^{2+}, 37.2 for Cu^{2+}, 40.2 for Pb^{2+} and 32.2 for Cd^{2+}.

Some $ML_{unknown}$ complexes cannot be destroyed at the electrode. For example, metal sulfide clusters and nanoparticles ranging from 0.50 to 3 nm size cannot be destroyed by anodic stripping pseudovoltammetry experiments (Luther III et al., 1999; Rozan et al., 2003; Tsang et al., 2006) as M_3S_3 (~0.50 nm, Luther III et al., 1999) and higher order clusters have log K_{therm} values exceeding 50. Fig. 4A shows pseudovoltammograms for Pb^{2+} in the surface, mid-depth and bottom waters of the Chesapeake Bay (modified from Rozan et al., 2003). The bottom water plot shows no 's' wave or current from M^{2+} reduction as free sulfide was 15 μM so outcompetes all organic ligands for the Pb^{2+}. However, the surface sample shows one $PbL_{unknown}$ complex (L_1) at −1.48 V whereas the mid-depth showed two weaker $PbL_{unknown}$ complexes (L_2,L_3) at −1.28 and − 1.05 V.

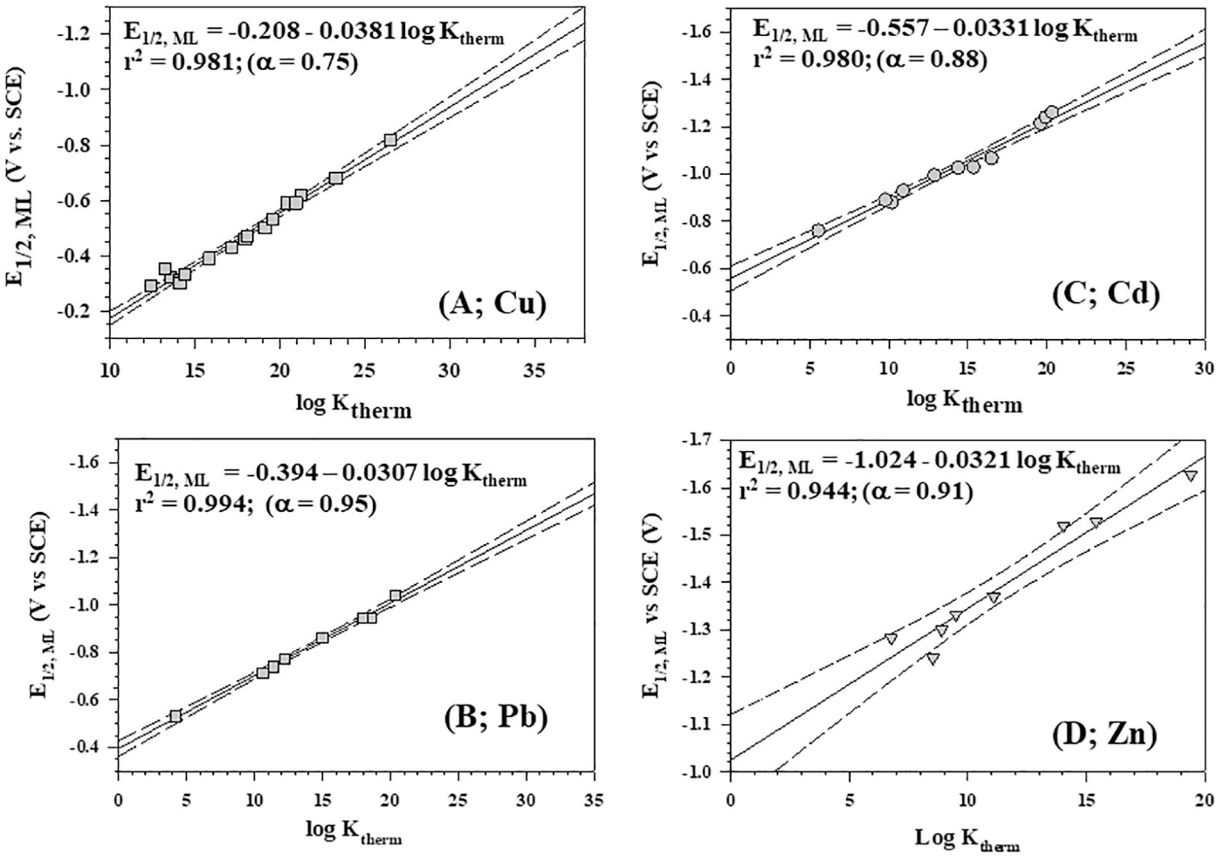

Fig. 3. Chelate scales for A) Cu^{2+}, B) Pb^{2+}, C) Cd^{2+} and D) Zn^{2+} (includes only inert complexes from Fig. 2B). The dashed lines in each indicate the 95% confidence limit. See Appendix Tables 5-7 for the data and Appendix Figs. 9–11 for the structures of the compounds. Note that the voltage scales differ because the working range varies based on the reduction potential of the free ion (M^{2+}).

On the addition of 1 nM Pb^{2+} to a surface sample containing 0.08 nM of only one strong $PbL_{unknown}$ complex (L_1) -1.48 V, Fig. 4B shows that the added Pb^{2+} reacts with three other unknown weaker ligands (L_2, L_3, L_4) in the sample at higher potentials that are in excess to L_1. Assuming a 1:1 ML complex, the concentration of the unknown ligands equals the increase in the measured M concentration between Fig. 4A and B. These data indicate that a CLE-CSV or ASV Pb^{2+} titration experiment would provide information mainly on the excess ligands (L_2, L_3, L_4) and not the actual ligand (L_1) binding Pb^{2+} in the sample.

Several workers (e.g., Baars and Croot, 2011; Croot et al., 2000; Kim et al., 2015, 2016; Nicolau et al., 2008; Rozan et al., 2003) showed that total metal concentrations in a sample can be higher than the sum of the concentrations for $ML_{unknown}$ complexes determined by pseudovoltammetry in some surface waters, which do not contain free sulfide. Thus, these samples have $ML_{unknown}$ organic complexes that are inert and cannot be destroyed at the electrode, so other methods are needed to determine those actual very strong $ML_{unknown}$ complexes in natural waters. Nevertheless, pseudovoltammetry experiments on natural waters provide much information on the nature of actual $ML_{unknown}$ complexes as well as excess ligands that can be titrated with M^{2+}.

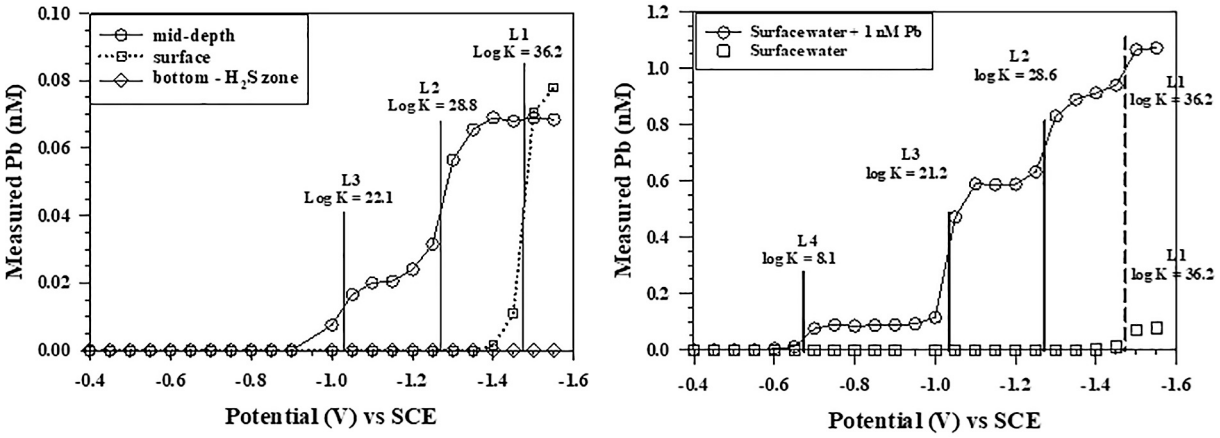

Fig. 4. A) Pseudovoltammograms of $PbL_{unknown}$ complexes from 3 different water masses of the Chesapeake Bay. B) Pseudovoltammogram of the surface water sample from Fig. 4A with and without the addition of 1 nM Pb^{2+}. Note the change in the y-axis scales between the figures.

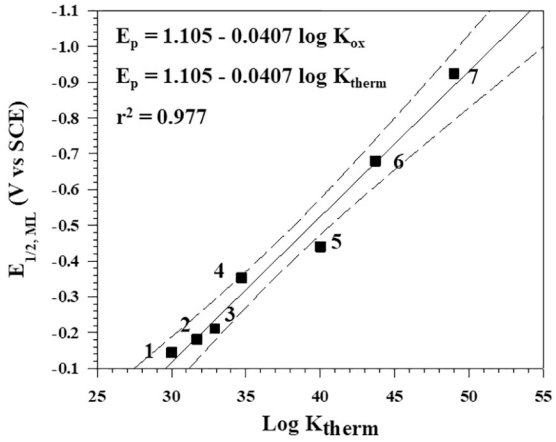

Fig. 5. Chelate scale for Fe(III) performed in bistris buffer (0.1 M NaCl, pH 7) with no deposition. The dashed lines in each indicate the 95% confidence limit. See the Appendix Table 8 for the data and Appendix Fig. 11 for the structures of the compounds.

4. Fe(*III*)L chelate scales

Unfortunately, in a seawater sample, the pseudovoltammetry approach cannot be used to directly provide information on K_{therm} for metals that do not form an amalgam. These metals include Fe(III), Co(II), Ni(II) and Mn(III), which must be experimentally determined by CLE-adCSV or spectrophotometric speciation methods. Thus, other approaches are needed to provide information beyond [L] and $K_{cond\ M'L'}$. Nevertheless, a FeL chelate scale has been determined at micromolar concentrations.

In these cases, there is reduction of a metal complex to a lower valency without metal-ligand dissociation as for Fe(III) in eq, 22. Formally, this reduction potential is determined by an adCSV experiment.

$$Fe^{3+}L + e^- \leftrightarrow Fe^{2+}L \tag{22}$$

$E_{½,\ ML}$ should be proportional to the ratio of the stability constants of the reduced [reaction of Fe^{2+} with L to form Fe(*II*)L] and oxidized complexes [reaction of Fe^{3+} with L to form Fe(*III*)L] and not just that of the oxidized reactant according to eq. 23, which is expanded to eq. 23a (Taylor et al., 1994).

$$E_{\frac{1}{2},ML} = E_{\frac{1}{2},\ M.matrix} - \frac{2.303\ RT}{\alpha nF}\ log\ \frac{K_{ox}}{K_{red}} \tag{23}$$

$$E_{\frac{1}{2},ML} = E_{\frac{1}{2},\ M.matrix} + \frac{2.303\ RT}{nF}\ log\ K_{red} - \frac{2.303\ RT}{nF}\ log\ K_{ox} \tag{23a}$$

K_{ox} and K_{red} are the thermodynamic stability constants of the oxidized (Fe^{3+}) and reduced (Fe^{2+}) forms of the complex, respectively. If the K_{red} values for all complexes are similar (for many $Fe^{2+}L$, log K_{therm} = 19), then the K_{red} term and α can be incorporated into the intercept (eq. 24):

$$E_{\frac{1}{2},ML} = intercept - \frac{2.303\ RT}{nF}\ log\ K_{ox} = intercept - \frac{2.303\ RT}{nF}\ log\ K_{therm} \tag{24}$$

As K_{ox} is the K_{therm} for the reaction of Fe^{3+} with L, these are pH independent constants for a given binding mode or structure. In this instance, the electrode processes are reversible (check by CV or SWV) because the complex does not dissociate or become destroyed, and $E_{½,\ ML}$ is independent of ligand concentration (check by titrating the metal with ligand until no further change in $E_{½,\ ML}$ is observed).

Taylor et al. (1994) and Lewis et al. (1995b) have used eq. 24 to develop and use a chelate scale (Fig. 5) to determine the K_{therm} for Fe(*III*)L complexes. The scale has ligands containing 0 to 3 catechol functional groups. This scale could be used for an unknown Fe(*III*)$L_{unknown}$ complex if the electrochemistry of the complex could be verified at low (sub) nanomolar concentrations via an adCSV experiment with deposition and no competitive ligand added. In fact, Laglera and van den Berg (2009) and Hassler et al. (2016) performed CSV experiments with deposition to detect and quantify humic substances bound to Fe(III) in a similar way. Unfortunately, ligands with hydroxamate functional groups do not conform to eq. 24, but ligands with β-hydroxyaspartate functional groups do (Holt et al., 2005). Nevertheless, Spasojević et al. (1999) have developed a scale based on hydroxamate functional groups that relates pFe with $E_{½,ML}$. Generally, the more negative the value for $E_{½,ML}$ correlates with higher denticity (larger number of ligating atoms) of the ligand. Knowledge of Fe(*III*)L reduction potentials is also important as some organisms use Fe(III)-reductases to acquire Fe(III) as Fe(II) from Fe(III) complexes. (e.g., Maldonado and Price, 2001).

5. Kinetic approach

5.1. Full recovery of the metal from an actual (natural) $ML_{unknown}$ in a sample to determine k_d (only)

There are few marine chemistry studies, which employ the stoichiometric mechanism approach outlined by Langford and Gray (1965), and Fe was the metal normally studied (e.g., Hudson et al., 1992; Wu and Luther III, 1995; Witter et al., 2000; Gerringa et al., 2007; Croot et al., 2011; Croot and Heller, 2012; Rose and Waite, 2003a; González et al., 2019). The following discussion is pertinent for any L_{comp} that is desired for use. The dissociation rate constant, k_d, can be determined using the steady state approximation from the associative reaction (eq. 25) to recover Fe from $FeL_{unknown}$ into L_{comp} to form FeL_{comp}. This process can be broken into *two elementary reaction steps*; the *dissociation* of the natural organic ligand complex to form Fe' (eq. 26), where Fe' represents the inorganic forms of Fe at ambient pH; and the *reaction* of Fe' with L_{comp} (eq. 27). As the method measures only FeL_{comp}, which has a specific reduction potential, there is no consideration of a mixed ligand or associative reaction that would form $FeL_{unknown}L_{comp}$.

$$FeL_{unknown} + L_{comp} \overset{k_{obs}}{\rightarrow} FeL_{comp} + L'_{unknown} \tag{25}$$

$$Fe' + L'_{unknown} \underset{k_d}{\overset{k_f}{\rightleftarrows}} FeL_{unknown} \tag{26}$$

$$Fe' + L_{comp} \overset{k_2}{\rightarrow} FeL_{comp} \tag{27}$$

The Fe' concentration will always be very small, and we can write the rate equation (eq. 28) for Fe' by applying the steady state approximation:

$$\frac{d}{dt}[Fe'] = 0 = k_d[FeL_{unknown}] - k_f[Fe'][L'_{unknown}] - k_2[Fe'][L_{comp}] \tag{28}$$

Solving for Fe', gives eq. 29:

$$[Fe'] = \frac{k_d[FeL_{unknown}]}{k_f[L'_{unknown}] + k_2[L_{comp}]} \tag{29}$$

Eq. 30 is the rate law for the formation of FeL_{comp} (eq. 27).

$$\frac{d}{dt}[FeL_{comp}] = k_2[Fe'][L_{comp}] = -\frac{d}{dt}[FeL_{unknown}] = k_{obs}[FeL_{unknown}] \tag{30}$$

Substituting eq. 29 for [Fe'] into eq. 30 gives eq. 31.

$$-\frac{d}{dt}[FeL_{unknown}] = \frac{d}{dt}[Fe(L_{comp})] = \frac{k_2[L_{comp}]\ k_d[FeL_{unknown}]}{k_f[L'_{unknown}] + k_2[L_{comp}]} \tag{31}$$

If $k_2[L_{comp}]$ is very large or $k_f[L'_{unknown}]$ is very small, the Fe' intermediate does not react readily with $L'_{unknown}$ to reform the reactant, $FeL_{unknown}$, and eq. 31 reduces to $k_{obs} = k_d$; thus, the rate depends on $[FeL_{unknown}]$ and Fe-$L_{unknown}$ bond breaking or dissociation. Typically,

the value of $k_2[L_{comp}]$ has been determined to be much greater than $k_f[L'_{unknown}]$. Thus, eq. 31 reduces to eq. 32.

$$-\frac{d}{dt}[FeL_{unknown}] = \frac{d}{dt}[FeL_{comp}] = \frac{k_2\ [\mathrm{Lcomp}]\ k_d[FeL_{unknown}]}{k_2[\mathrm{Lcomp}]} = k_d[FeL_{unknown}] \quad (32)$$

After integrating, eq. 32 becomes eq. 33.

$$ln[FeL_{unknown}] = -k_d t = -k_{obs}[L_{comp}]t \quad (33)$$

A plot of ln $[FeL_{unknown}]$ versus time allows calculation of k_d. Section 5.2 and Fig. 6 show an example.

When $k_2[L_{comp}]$ and $k_f[L'_{unknown}]$ have similar values, the full form of k_{obs} is eq. 34 (from comparing eqs. 31 and 32).

$$k_{obs} = \frac{k_2 k_d[L_{comp}]}{k_f[L'_{unknown}] + k_2[L_{comp}]} \quad (34)$$

5.2. General procedure for recovery of a metal from $ML_{unknown}$

To perform a recovery experiment, L_{comp} is added to a sample and ML_{comp} is detected over time. Fig. 6a shows an experiment with 7 data points. To determine k_d values for more than one $ML_{unknown}$ complex in a sample, more data points are needed. Typically, ~10 mL of sample are needed to assay for ML_{comp}. To achieve 20 data points, the desired concentration of L_{comp} can be added to 200 mL of sample in a trace metal cleaned bottle so that 10 mL aliquots can be taken for measurement at convenient times. The experiment is done at the natural pH of the sample, and any reagents that are needed for the ML_{comp} assay are added only at the time of measurement in the voltammetry cell.

Madison et al. (2011) provided an example for micromolar concentrations of Mn(*III*)$L_{unknown}$ complexes in porewaters where a diode array UV–Vis spectrophotometer was used to collect data points every 6 s over 15 min by continuously monitoring the formation of Mn(*III*)L_{comp} after addition of L_{comp} to the sample in the cuvette.

5.3. Partial recovery of the metal from $FeL_{unknown}$ with achievement of equilibrium. Determination of 4 parameters in a sample: $K_{condML'}$, $K_{condM'L'}$, k_d and k_f

f less L_{comp} is added so as not to obtain 100% recovery of Fe from $FeL_{unknown}$, then equilibrium is achieved between $FeL_{unknown}$ and FeL_{comp}. It is now possible to calculate $K_{recovery}$ (eq. 35) from the mass balance of the following eq. 25a (related to eq. 25 above). For strong $FeL_{unknown}$ complexes, the assumption is a 1:1 stoichiometry of Fe and $L_{unknown}$. However, many competitive ligands are bidentate ligands which bind Fe to form complexes of form $Fe(L_{comp})_x$ where x can be 2 or 3. For ligands that are quadridentate and higher x is 1.

$$Fe^{3+} + L_{unknown} + x\ L_{comp} \rightleftarrows Fe^{3+}(L_{comp})_x + L'_{unknown} \quad (25a)$$

$$K_{recovery} = \frac{[Fe^{3+}L_{comp}][L'_{unknown}]}{[Fe^{3+}L_{unknown}]\ [L_{comp}]^x} \quad (35)$$

Eq. (36) Relates $K_{recovery}$ to the conditional thermodynamic constants, $K_{FeLcomp'}$ and $K_{FeLunknown'}$.

$$K_{recovery} = \frac{[Fe^{3+}L_{comp}]\ [Fe^{3+}]\ [L'_{unknown}]}{[Fe^{3+}L_{unknown}]\ [Fe^{3+}]\ [L_{comp}]^x} = \frac{K_{FeLcomp'}}{K_{FeLunknown'}} \quad (36)$$

Because these metal-ligand complex equations are a function of the free metal ion concentration, these conditional constants ($K_{cond\ ML'}$) are already corrected for the side reaction coefficient of the metal. Thus, if calculations described in section 5.1 (eq. 33) and eq. 36 are performed from the same experiment, the value of k_f can be evaluated from eqs. 10 and 10a as $K_{condML'}$ and k_d can be determined from the same experiment; also, $\alpha_{Fe'}$ is known (10^{10}, Hudson et al., 1992). Likewise, $K_{cond\ M'L'}$ can be calculated from the same equation.

$$logK_{cond\ ML'} = logK_{cond\ M'L'} + log\alpha_{M'} = logk_f - logk_d + log\alpha_{M'} \quad (10a)$$

thus, $logk_f = logK_{cond\ ML'} + logk_d - log\alpha_{M'}$

and $logK_{cond\ M'L'} = logK_{cond\ ML'} - log\alpha_{M'}$

To demonstrate these relationships, Fig. 7A shows data from Wu and Luther III (1995) regarding the recovery of Fe from $FeL_{enterobactin}$ with the competitive ligand 1N2N. $FeL_{enterobactin}$ was formed by the reaction of 7 nM Fe(III) added to 20 nM of enterobactin in seawater. At equilibrium (after 60 h), the concentrations were $[FeL_{enterobactin}] = 3 \times 10^{-9}$ M, $[L_{enterobactin}] = 17 \times 10^{-9}$ M, $[FeL_{1N2N}] = 4 \times 10^{-9}$ M and $[L_{1N2N}] = 1.36 \times 10^{-5}$ M. Using eq, 25a with x = 3, $K_{recovery}$ was calculated as 9.01×10^6.

$$K_{recovery} = \frac{[Fe^{3+}(1N2N)_3][ent]}{[Fe^{3+} - ent]\ [1N2N]^3} = \frac{K_{Fe(1N2N)3'}}{K_{Fe-ent'}} = 9.01\ x\ 10^6$$

As $K_{Fe(1N2N)3'} = 6.31 \times 10^{27}$, $K_{Fe\text{-}ent'}$ is calculated to be 7.00×10^{20} or $\log K_{Fe\text{-}ent'} = 20.84$. As noted in section 5.1, Fig. 7B shows the calculation of k_d for the $Fe^{3+}L_{ent'}$ complex using the first 5 data points. Thus, k_d and $\log k_d$ are evaluated to be 3.80×10^{-6} s^{-1} and -5.42, respectively. From eq. 10a, k_f and $\log k_f$ are calculated to be 2.63×10^5 M^{-1} s^{-1} and 5.42, respectively (see section 5.4 for experimental methods to determine k_f). Thus, $\log K_{Fe'\text{-}ent'} = 10.84$. These calculations indicate that an equilibrium experiment can provide all the information needed to determine $K_{Fe\text{-}ent'}$, $K_{Fe'\text{-}ent'}$, k_f and k_d; a fifth parameter, $\alpha_{M'}$, is known. Thus, 5 of 7 unknown parameters in eq. 13 (13a) can be determined in one experiment.

The only 2 terms not known from eq. 13 are $\log K_{therm}$ and $\log \alpha_L$, which are in bold font below. Witter et al. (2000) evaluated k_f (from section 5.4) and k_d (from section 5.1) for several Fe(III)-siderophore complexes in Table 3. Here, we used those kinetics data, the known $\alpha_{Fe'}$ and known K_{therm} values to calculate their $\log \alpha_{L'}$ values (see Table 3).

$$logK_{therm} = logK_{cond\ M'L'} + log\alpha_{M'} + \mathbf{log\ \alpha_{L'}} = logk_f - logk_d + log\alpha_{M'} + \mathbf{log\ \alpha_{L'}} \quad (13)$$

Because $K_{cond\ ML'}$ can be evaluated as above, eq. 13 is rearranged to eq. 13a.

$$logK_{therm} - log\alpha_{L'} = logK_{cond\ ML'} = logk_f - logk_d + log\alpha_{M'} \quad (13a)$$

$$or\ log\alpha_{L'} = logK_{therm} - logk_f + logk_d - log\alpha_{M'}$$

Many oceanographers perform CLE-CSV experiments to obtain $K_{cond\ M'L'}$ once a $L_{unknown}$ is isolated from a sample by chromatography with mass spectrometry detection (e.g., Bundy et al., 2018). However, more information can be ascertained as $\log \alpha_{L'(H\ only)}$ can be calculated from an acid-base titration in a sodium chloride solution to obtain the protonation or acid dissociation constants for $L_{unknown}$ (see eqs., 2a, 5a and 8a). Reid et al. (1993) calculated K_{therm} for the Fe(*III*)alterobactin-A complex in this manner from eq. 14 after performing equilibrium $K_{recovery}$ experiments between Fe(*III*)EDTA and Fe(*III*)alterobactin-A in varying concentrations of each ligand to determine $K_{Fealt\text{-}A'}$ (from eq. 36 for $K_{cond\ ML'}$). In their experiments, ML concentrations were followed by their characteristic UV–Vis peaks.

$$logK_{therm} = logK_{cond\ ML'} + log\alpha_{L'(H\ only)} \quad (14)$$

If not enough material can be isolated by chromatography with mass spectrometry detection for complete structural analysis and determination of $\log \alpha_{L'(H\ only)}$, the functional group(s) can be determined. For example, Boiteau et al. (2019) isolated and identified several siderophores containing hydroxamate groups from seawater samples as well as siderophores that were not identified. The isolated $L_{unknown}$ can be reacted with Fe(III) to determine $\log K_{therm}$ from the Fe(III) chelate scales for catecholate and β-hydroxyaspartate functional groups (Taylor

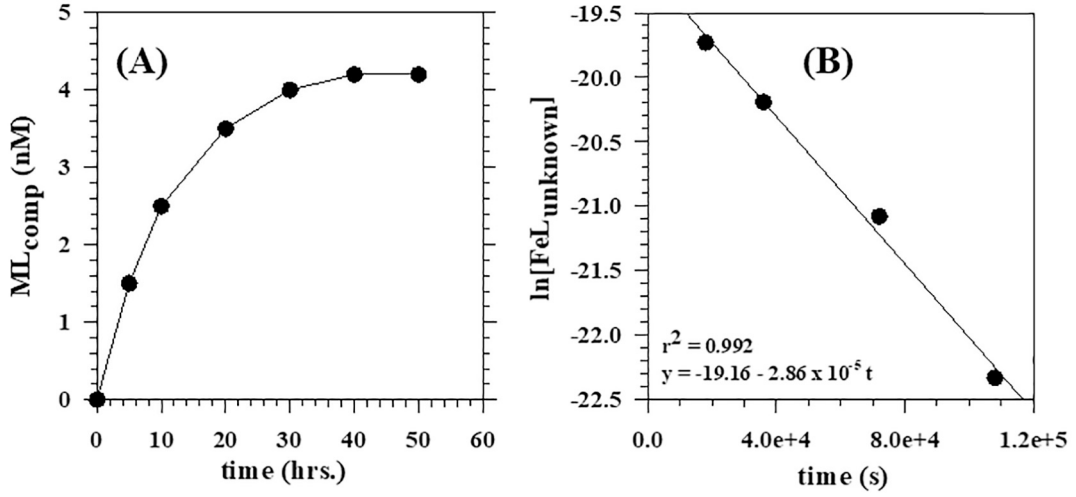

Fig. 6. Recovery of Fe from $FeL_{unknown}$ using a competitive ligand, L_{comp}. In Fig. 6B, e+4 and e+5 indicate 10^4 and 10^5.

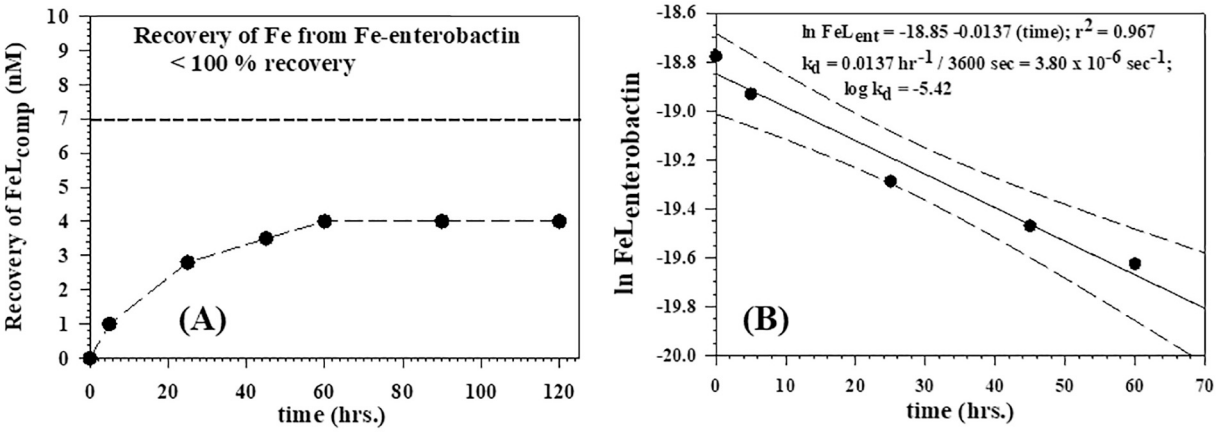

Fig. 7. A) Recovery of Fe^{3+} in the Fe^{3+}enterobactin complex using 1N2N as the competitive ligand; horizontal line indicates the Fe added. B) Linearization of the first 5 points (before equilibrium is reached) is used to calculate k_d for the $Fe^{3+}L_{ent'}$ complex; dashed lines indicate 95% confidence limits.

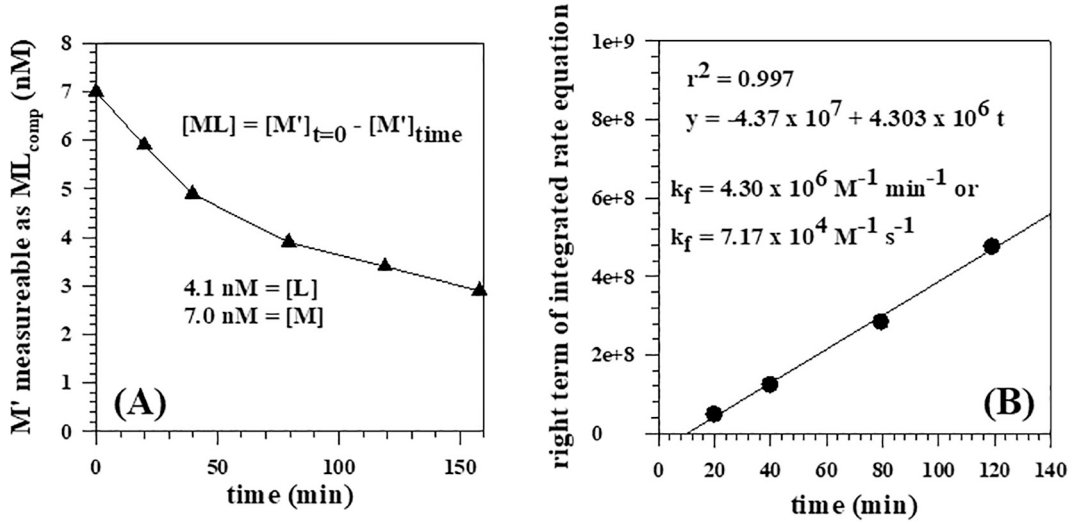

Fig. 8. A) Determination of M′ after addition of excess Fe' (7 nM total) to a sample from the NW Atlantic Ocean (sample from Witter and Luther III, 1998) containing 4.1 nM excess ligand; each time point represents a separate aliquot from a sample previously treated with the competitive ligand. B) Integrated rate equation for a second order reaction versus time to determine k_f; points 2–5 are used for the calculation as the first data point indicates the addition of Fe' and not an experimentally determined value.

et al., 1994) or for hydroxamate functional groups (Spasojević et al., 1999). If desired, both log $K_{cond\ ML'}$ and log K_{therm} are now known so log $\alpha_{L'}$ can be calculated from eq. 14a once a separate experiment is performed to form $FeL_{unknown}$ and determine $K_{cond\ ML'}$ in seawater.

$$log\alpha_{L'} = logK_{therm} - logK_{cond\ ML'} \quad (14a)$$

Similarly, obtaining $\alpha_{L'}$ for an unknown ligand in $ML_{unknown}$ for Cu^{2+}, Zn^{2+}, Cd^{2+}, Pb^{2+} is possible by performing 2 experiments and without isolating the $L_{unknown}$. First, a pseudovoltammogram can be performed on the sample to give log K_{therm}. Second, a kinetics experiment as in this section can be performed to follow the loss of every 's' wave in the pseudovoltammogram (e.g., Fig. 4A) with a competitive ligand and/or the increase of a ML_{comp} peak until equilibrium is attained to measure $K_{recovery}$. Thus, log $K_{cond\ ML'}$ can be obtained from eq. 36, and log $\alpha_{L'}$ calculated from eq. 14a. Many values of log $\alpha_{L'}$ in Table 3 were determined by this approach. The value of log $\alpha_{L'}$ for a $L_{unknown}$ can be compared to known ligand values (Table 3) to give information on the type of functional group(s) binding the metal. Thus, for Cu^{2+}, Zn^{2+}, Cd^{2+}, Pb^{2+}, only two experiments (section 3 and this section) are needed to determine all 7 parameters in eqs. 13, 13a.

5.4. Determination of the rate of formation, k_f, of ML (for xs $L_{unknown}$ in a sample or for a L_{known} that has been isolated from the sample or a culture)

Unfortunately, the k_f of a natural $ML_{unknown}$ complex cannot be obtained unless the $L_{unknown}$ can be isolated and reacted with Fe'. However, natural samples contain excess $L'_{unknown}$ (or several) to the total Fe; thus, k_f of those $ML_{unknown}$ complexes can be experimentally determined in addition to the value calculated from experiments in section 5.3 (eq. 10a). The formation of an ML complex is a second order reaction (eqs. 37a, b).

$$M' + L' \xrightarrow{k_f} ML \quad (37a)$$

$$\frac{d}{dt}[ML] = k_f[M'][L'] \quad (37b)$$

The kinetics can be determined by adding a small ***excess*** M′ to a solution or sample containing xs $L'_{unknown}$ in seawater (or the medium of interest) and determining M′ over time (by taking an aliquot of the sample and reacting with L_{comp}).

5.5. General procedure for k_f determination

The desired concentration of M′ can be added to 200 mL of sample in a trace metal cleaned bottle so that 10 mL aliquots can be taken for measurement at convenient times. For Fe(III), it is important to add Fe at a slight excess (< 50%) to the concentration of the excess ligand in the sample to avoid formation of iron colloids that can react with the competitive ligand; thus, complicating the interpretation of the experimental data. The experiment is again done at the natural pH of the sample. L_{comp} and any other reagents that are needed for the ML_{comp} assay are added to the aliquot only at the time of measurement in the voltammetry cell.

Fig. 8A shows a plot of the loss of [M′] over time as $ML_{unknown}$ forms. In this case, M′ is detectable as ML_{comp}, but the complex $ML_{unknown}$, which forms rapidly, is not detectable because the L_{comp} is added to an aliquot of the solution and run quickly after the aliquot is taken (L_{comp} has little time to compete with $ML_{unknown}$). In Fig. 8B, the integrated rate expression, eq. 38, can be used to calculate the second order rate constant k_f from a plot of t versus the entire right side of eq. 38, which gives a straight line.

$$k_f t = \frac{1}{[M'_0] - [L'_0]}\ x\ ln\left\{\frac{[L'_0]([M'_0] - [ML])}{([L'_0] - [ML])[M'_0]}\right\} \quad (38)$$

M'_0 and L'_0 indicate the initial concentrations of M′ and $L'_{unknown}$. As [ML] = 0 at time 0, total $[L'_0]$ for a 1:1 complex is the difference between the [M′] added minus the [M′] measured at the end of the experiment. Fig. 8 is an example of the reaction rate for oxidized Fe' with an excess $L'_{unknown}$. If $L'_{unknown}$ can be isolated from the sample by chromatographic methods and its structure determined, it becomes L_{known}. Likewise, M′ can be added to a L_{known} solution to determine the k_f of ML_{known}.

6. Brief comments on filtration and reactivity

Researchers have typically used 0.2 or 0.4 μm filters to separate suspended particles prior to trace metal analysis. However, 20 nm and 3–10 KDa filters (Sañudo-Wilhelmy et al., 1996; Schlosser and Croot, 2008) have been used to separate colloidal material that passes through the 0.2 or 0.4 μm filters. As a result, some researchers indicate that the material coming through these smaller filters is "truly dissolved" (e.g., Fitzsimmons and Boyle, 2014; Fitzsimmons et al., 2014; Gerringa et al., 2016). Classification of a chemical species as "truly dissolved" when passing through 20 nm filters is not favored terminology as size does not determine reactivity at an electrode or during metal uptake by an organism. We now provide examples.

The size classification of nanoparticles ranges from 1 to 100 nm (Hochella et al., 2019); thus, nanoparticles can pass through 20 nm filters. However, molecules and nanoparticles smaller than the filter or ultrafilter size may not all pass through the filter due to their polarizability and interaction with the membrane (Schlosser and Croot, 2008) or due to clogging of pores by larger particles (Yücel et al., 2011). Also, a nanoparticle containing 500 Pb and 500 S atoms has a diameter (size) of 2.62 nm with a length of 1.515 nm, a volume of 3.48 nm^3, and a molecular mass of 119.6 kD (Luther, 2016), which can pass a 20 nm filter; however, it is not electroactive in a pseudovoltammetry experiment (Rozan et al., 2003).

In contrast, Taylor et al. (1994) observed that Fe(III) bound to the numerous catechol groups (15 mol% of total amino acids; Zeng et al., 2010) in the >100 kDa foot protein of *Mytilus edulis* are reduced to Fe (II)-catechol at the Hg electrode. The minimum diameter of a 100 kDa protein is 3.05 nm (Erickson, 2009). Thus, despite the similarity in molecular mass and size with the 2.62 nm PbS nanoparticle, these chemical species have entirely different reactivity. The protein would be considered "truly dissolved', but the PbS nanoparticle would not.

Two examples of smaller complexes, which behave like the protein and could be considered 'truly dissolved', are provided. A decapeptide, which contains 2 ligating atoms, is on the order of 1 kDa. Thus, when 2 decapeptides complex a single metal ion, which acts as a cross linking material, the molecular mass doubles to 2 KDa plus the mass of the metal. A siderophore bound to a metal can have as many as 6 ligating atoms binding a metal ion. Siderophores and their metal complexes commonly have a molecular mass ≤ 1 kDa. From Erickson (2009), a 1 kDa complex has a minimum size of 0.66 nm and a 3 kDa complex a size of 1 nm. In summary, the size of a chemical constituent does not convey information regarding its reactivity, which is more important than describing whether a constituent is dissolved or not.

We note that Purawatt et al. (2007) found that phytic acid (*myo*-insitol hexakisphosphate, a major component of eukaryotic cells) reacts with Fe(III) to form colloidal material in the 1–500 kDa size range at pH 7. The phosphate groups likely act as bridging groups to bind with and increase Fe(III) solubility. This behavior is different from that described above for the foot protein of *Mytilus edulis*. These data and the crossflow ultrafiltration work of Schlosser and Croot (2008) on the Fe-phytic acid system were done at total Fe concentrations that were an order of magnitude higher than a previous study by Witter et al. (2000), but indicate that phytic acid is not a strong Fe(III) chelator.

7. Suggested protocols for analysis of ML complexes in samples

Appendix Fig. 12 is a flow chart for the protocols and variables, which can be measured, that are described in the next two sections.

7.1. Metals that form an amalgam for which a 'chelate scale' has been developed

Two voltammetry experiments can provide information on all 7 ML parameters.

(1) For complexes of Cu^{2+}, Zn^{2+}, Cd^{2+} and Pb^{2+}, the K_{therm} can be obtained via a pseudovoltammetry experiment (section 3).
(2) A kinetics experiment to achieve equilibrium with a competitive ligand to form and measure ML_{comp} as in section 5.3 provides $K_{cond\ ML'}$ (eq. 36) and k_d (eq. 33); $K_{cond\ M'L'}$ and k_f can then be calculated by eq. 10a. As $\alpha_{M'}$ is known for these metals, $\alpha_{L'}$ can be calculated from eq. 14a.

If there is more than one natural ligand bound to the metal, several pseudovoltammetry experiments would be needed to follow the kinetics of these 's' waves by following the decrease in current (concentration) of each $ML_{unknown}$ rather than measuring the ML_{comp} signal alone. Adding a competitive ligand to follow the original waves would allow following the loss of current for each unknown ML complex via pseudovoltammetry at each time point. Because ML_{comp} may have its own wave, it should not be added in too much excess as the wave may interfere with the $ML_{unknown}$ waves; thus, a siderophore with six ligating atoms might be useful. Once equilibrium is achieved, then $K_{recovery}$ (eq. 35), $K_{cond\ ML'}$ (eq. 36) and k_d (eq. 33) can then be determined as in section 5.3; $K_{cond\ M'L'}$ and k_f can then be calculated by eq. 10a. As $\alpha_{M'}$ is known for these metals, $\alpha_{L'}$ can be calculated from eq. 14a. For $ML_{unknown}$ complexes that are fully recovered, only k_d (section 5.1, eq. 33) can be determined. Several (4–7) pseudovoltammetry experiments at different time points would be needed to follow the kinetics of each of these waves.

Also, kinetics experiments can be performed on excess ligands by adding the metal to the sample and doing a second series of pseudovoltammetry experiments (Figs. 1C, 4B) to follow the increase in current for each 's' wave representing an individual $ML_{unknown}$. If the reactions are not too fast, k_f can be evaluated for each complex using eq. 38 in section 5.4. After all excess $ML_{unknown}$ complexes form to completion, a competitive ligand can be added to determine the recovery of every $ML_{unknown}$ complex into ML_{comp} by following the decrease in current for each $ML_{unknown}$ wave with time simultaneously. Calculations can then be performed as noted at the end of the previous paragraph.

7.2. Metals that are reduced to a lower valency at the electrode (do not form an amalgam)

Fe(III) and many other metals are in this category, but all metals can be determined using this approach. We describe two separate methods to determine the 7 parameters for ML complexes.

First, one voltammetry kinetics experiment on the sample and an isolation of the ligand to determine its protonation or acid dissociation constants followed by a second voltammetry kinetics experiment are needed.

(1) A kinetics experiment to achieve equilibrium with a competitive ligand in seawater as in section 5.3 provides $K_{cond\ ML'}$ (eq. 36) and k_d (eq. 33); $K_{cond\ M'L'}$ and k_f can then be calculated by eq. 10a (section 5.3). Although $\alpha_{M'}$ is known for these metals, $\alpha_{L'}$ cannot be calculated unless the ligand is isolated.
(2) Upon isolation and characterization of the ligand ($L_{isolated}$ or L_{known}), the protonation or acid dissociation constants of the ligand can be determined to give $\alpha^{j-}_{H_n\ ligand}$ and $\alpha_{L'(H\ only)}$ in a non-complexing medium (e.g. sodium chloride, see eqs. 2a, 5a and 8a).
(3) Reacting the isolated ligand with the metal in seawater as outlined in section 5.5 forms $ML_{isolated}$; then, use of eq. 38 provides k_f, which can be compared with the calculated value of k_f in the first experiment. Using this solution upon complete reaction to form $ML_{isolated}$, a second kinetics experiment to achieve equilibrium with a competitive ligand as in section 5.3 provides $K_{cond\ ML'}$ (eq. 36) and k_d (eq. 33). K_{therm} is then evaluated using eq. 14 (section 5.3).

To calculate $\alpha_{L'}$ in seawater (see eqs. 2b, 5b and 8b), $K_{cond\ ML'}$ from experiment 1 and K_{therm} from experiment 3 are used in eq. 14a.

Second, if a chelate scale is available as for Fe(III)-ligands (section 4.0), one voltammetry kinetics experiment on the sample and an isolation of the ligand prior to performing a second voltammetry experiment using the chelate scale data are needed.

(1) A kinetics experiment to achieve equilibrium with a competitive ligand in seawater as in section 5.3 provides $K_{cond\ ML'}$ (eq. 36) and k_d (eq. 33); $K_{cond\ M'L'}$ and k_f can then be calculated by eq. 10a (section 5.3).
(2) Upon isolation of the ligand, the ligand is reacted with the metal to form $ML_{isolated}$ in the solution matrix that is used to generate the 'chelate scale;' and K_{therm} determined. The $\alpha_{L'}$ in seawater is then calculated using eq. 14a (section 5.3).
(3) If desired, react the isolated ligand with the metal in seawater as outlined in section 5.5 to form $ML_{isolated}$; use of eq. 38 provides k_f, which can be compared with the calculated value of k_f in the first experiment.

In contrast to the pseudovoltammetry protocol in section 7.1, isolation of the ligand is required to obtain all seven ML parameters for these metals. Also, after isolating a ligand, a separate kinetics experiment to determine $K_{cond\ ML'}$ (eq. 36) and k_d (eq. 33) is needed to show that the isolated ligand is the natural ligand initially determined in the sample experiment (1) for both methods above.

Obviously, a CLE-CSV metal titration experiment can be performed. This provides the total ligand concentration [L] and the conditional stability constant, $K_{cond\ M'L'}$, of the metal unknown ligand complex, $ML_{unknown}$. However, this information may be primarily for excess unknown ligands as shown in the metal addition experiment of Fig. 4B. A second separate kinetics experiment to obtain $K_{cond\ ML'}$ and k_d can be performed from which k_f can be calculated. A third experiment is needed to determine either K_{therm} or $\alpha_{L'}$.

8. Note concerning electrode materials, detection limits and adsorption artefacts

For samples from some oligotrophic regions, trace metal concentrations may be too low so HMDE experiments may not be sensitive enough to perform pseudovoltammetry experiments. Vibrating electrode methods (Gibbon-Walsh et al., 2012; Bi et al., 2013) have excellent detection limits so could be used, but the upper limit for the determination of K_{therm} values will be about one-half of the Log K value of HMDE experiments. Glassy-carbon rotating disk electrodes (RDE) with a thin Hg film also have excellent detection limits but have not been used for the determination of a 'chelate scale'. Lewis et al. (1995a, 1995b) noted that RDEs are susceptible to adsorption artefacts from organic material in coastal waters whereas such artefacts are not a problem in open ocean waters (Bruland, 1989). Nevertheless, Bi et al. (2013) note that proper conditioning of the electrode can prevent organic matter adsorption artefacts in coastal waters. Recently, Pađan et al. (2021) added Triton_X-100 to seawater samples and found that this prevented adsorption artefacts when analyzing for Cu speciation.

There have been many improvements in detection limits for competitive ligand work that can be applied to kinetics experiments, and we note the ligands TAC (2–2(2-thiazolylazo)-*p*-cresol) by Croot and Johansson (2000) and DHN (dihydroxynapthalene) by van den Berg (2006).

As we prepared this manuscript, we also found that pH, pH scale and temperature of speciation analyses were not always specified in detail.

9. Other analytical methods

Trace metal concentrations can also be determined by other methods. UV–Vis methods have been used to determine information on known Fe(*III*) L complexes (e.g., Reid et al., 1993; Rose and Waite, 2003b) and unknown Mn(*III*)L complexes (e.g., Luther III et al., 2015) at micromolar levels. Liquid core waveguides that are 1 to 5 m in path length can be used to determine (sub)nanomolar concentrations depending on the molar absorptivity of the ML_{comp} complex (e.g., Waterbury et al., 1997 for Fe(II); Thibault de Chanvalon and Luther III, 2019 for Mn(III)). The data from these and other methods (e.g., HPLC-ICP-MS) can be combined with the equations above to determine the 7 ML thermodynamic, kinetic and speciation parameters (K_{therm}, $K_{condML'}$, $K_{condM'L'}$, k_f, k_d, $\alpha_{M'}$, $\alpha_{L'}$). The experimental procedures would be those described in the first part of section 7.2.

Declaration of Competing Interest

None.

Acknowledgements

This work was supported by grants from the Chemical Oceanography (OCE-1558738) and the Marine Geology Geophysics (OCE-1558712) programs of the National Science Foundation. We thank V. Oldham for reviewing an earlier version of the manuscript. We thank Peter Croot and two anonymous reviewers for their constructive comments to improve the manuscript.

Appendix A. Appendix Tables

Appendix Table 5
Data used to generate the Cu^{2+} chelate scale. K_{therm} data from Martell and Smith (1974, 1977, 1982, 1986); $T = 25$ °C and corrected for the ionic strength of seawater.

Ligand, stoichiometry	log K_{therm}	$E_{1/2,\ ML}$
UV seawater		−0.25
NTA, CuL	12.37	−0.29
DFOB, CuL	13.35	−0.32
1,5,9- triazacyclododecane, CuL	13.2	−0.35
dopamine, CuL	14.04	−0.31
benzoylacetome, CuL_2	14.10	−0.30
DOPA, CuL	14.4	−0.33
1,4,7-triazacyclononane,CuL_2	15.84	−0.39
NTA,CuL_2	17.13	−0.43
EDTA,CuL	17.94	−0.46
Dimethylglyoxime,CuL_2	18.05	−0.47
Nioxime,CuL_2	19.11	−0.50
Ethylenediamine, CuL_2	19.60	−0.53
DTPA, CuL	20.43	−0.59
CDTA, CuL	21.24	−0.62
Trien (2,2,2-tet), CuL	20.97	−0.59
cyclen, CuL	23.3	−0.68
cyclam, CuL	26.50	−0.82

Appendix Table 6
Data used to generate the Pb^{2+} chelate scale. K_{therm} data from Martell and Smith (1974, 1977, 1982, 1986); T = 25 °C and corrected for the ionic strength of seawater.

Organic ligand, stoichiometry	log K_{therm}	$E_{1/2,\ ML}$
Oxalate, PbL	4.2	−0.531
Glutamate, PbL	10.6	−0.711
NTA, PbL	11.4	−0.740
Cysteine, PbL	12.21	−0.771
Glutamate, PbL_2	15.0	−0.860
Cysteine, PbL_2	18.57	−0.944
EDTA, PbL	18.0	−0.946
CDTA, PbL	20.38	−1.040

Appendix Table 7
Data used to generate the Cd^{2+} chelate scale. K_{therm} data from Martell and Smith (1974, 1977, 1982, 1986).

Ligand, stiochiometry	log K_{therm}	$E_{1/2,\ ML}$

(*continued on next page*)

Appendix Table 7 (*continued*)

Ligand, stiochiometry	log K_{therm}	$E_{1/2,\ ML}$
Salicylic acid, CdL	5.55	−0.760
Glutathione, CdL	10.18	−0.880
NTA, CdL	9.78	−0.890
penicillamine, CdL	10.90	−0.930
cysteine, CdL	12.88	−0.995
NTA, CdL_2	14.39	−1.026
Glutathione, CdL_2	15.35	−1.029
EDTA, CdL	16.50	−1.067
Cysteine, CdL_2	19.60	−1.213
CDTA, CdL	19.93	−1.240
Penicillamine, CdL_2	20.33	−1.260

Appendix Table 8
Data used to generate the Fe(III) chelate scale. Ent = enterobactin. All data from Taylor et al. (1994).

Complex, data # for Fig. 5	pH	$E_{1/2,\ ML}$	Log K_{therm}
$[FeCDTA]^-$, 1	7	-0.145	30.0
$[FeNTAtiron]^-$, 2	7	-0.182	31.7
$[FeNTAcat]^{2-}$, 3	7	-0.211	32.9
$[Fe(cat)_2]^-$, 4	7	-0.354	34.7
$[Fe(4Ncat)_3]^{3-}$, 5	7	-0.440	40.0
$[Fe(cat)_3]^{3-}$, 6	10	-0.680	43.7
$[Fe\text{-}ent]^{3-}$, 7	7	-0.924	49.0

Appendix B. Appendix figures

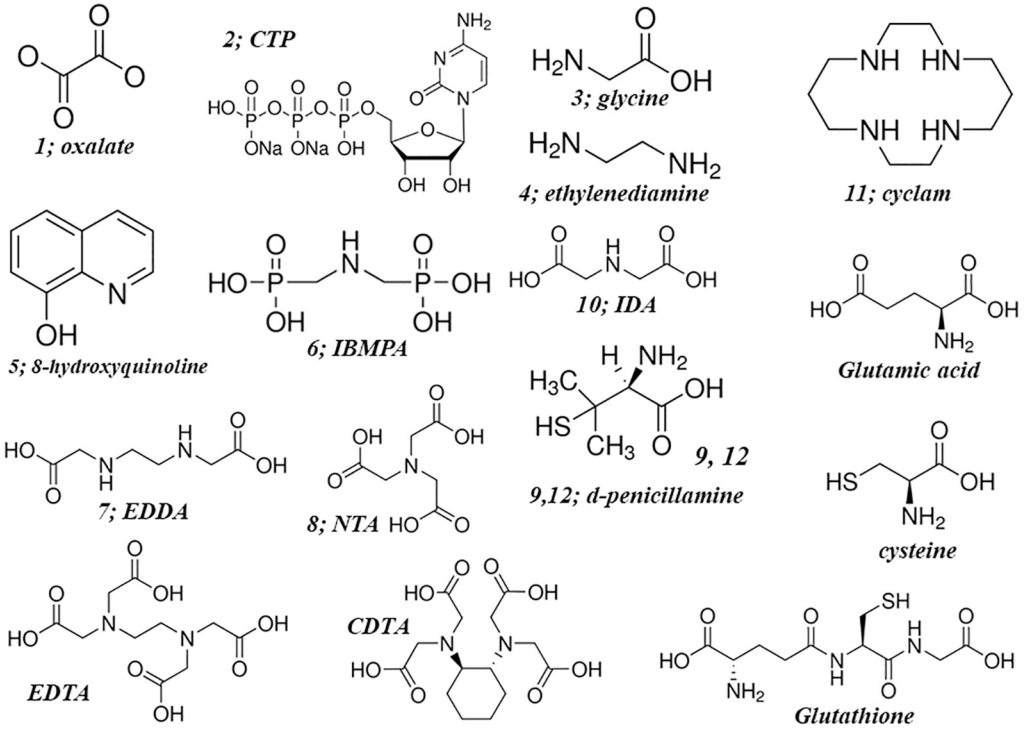

Appendix Fig. 9. Structures of model ligands for the Zn chelate scale plus others used for the Cd and Pb chelate scales.

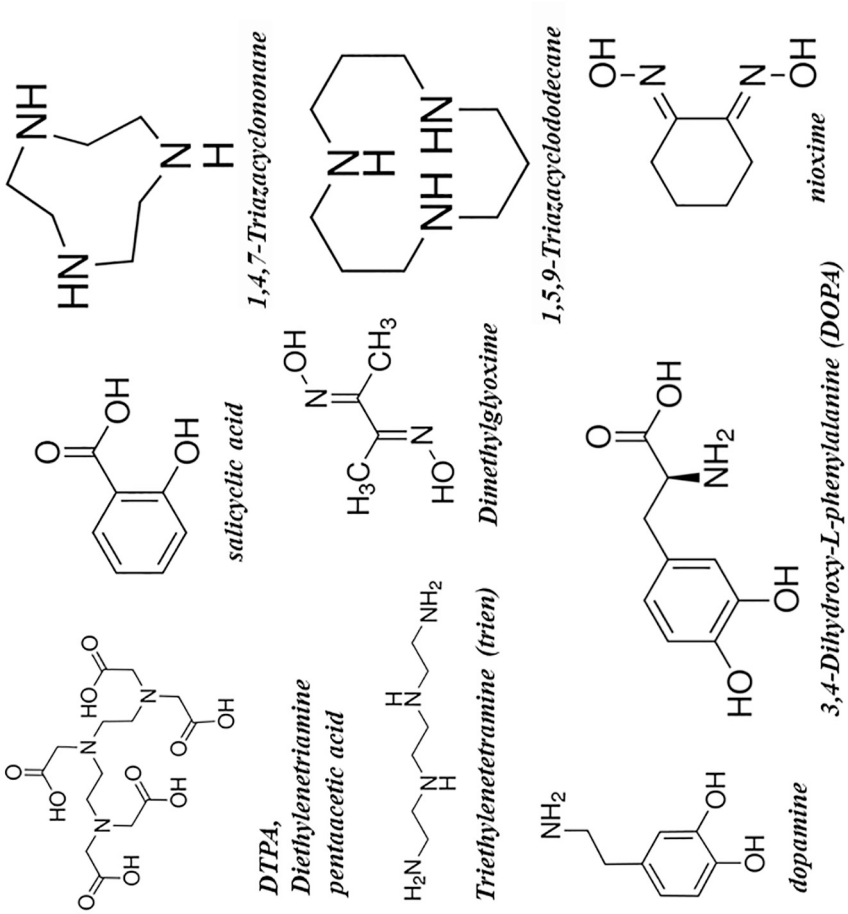

Appendix Fig. 10. Additional structures of model ligands for the Cu chelate scale.

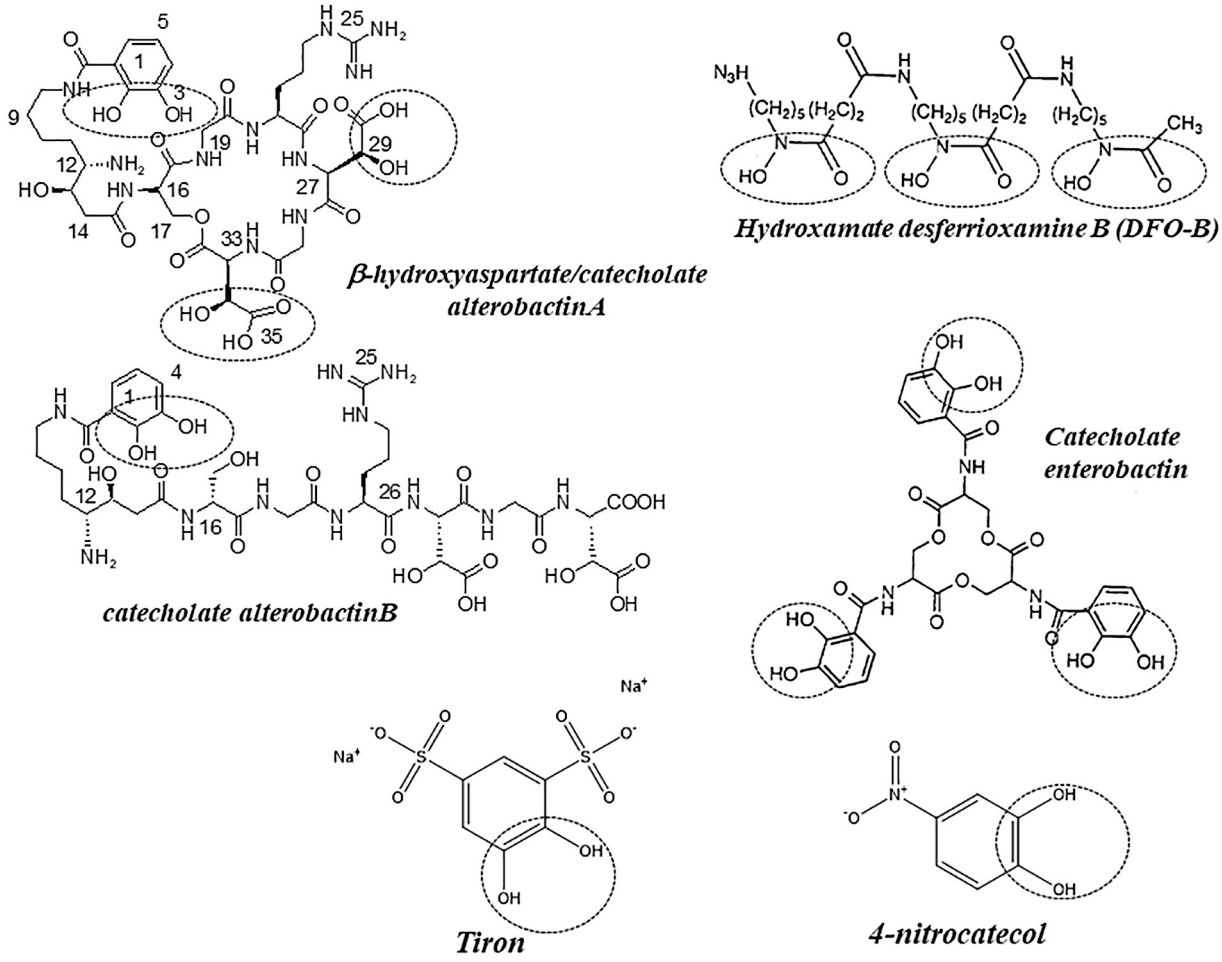

Appendix Fig. 11. Structures of model ligands for the Fe(III) chelate scale include catechol and β-hydroxasparate functional groups. DFO-B has hydroxamate functional groups and was used to generate the Cu chelate scale. Functional groups are in dashed circles or ellipses.

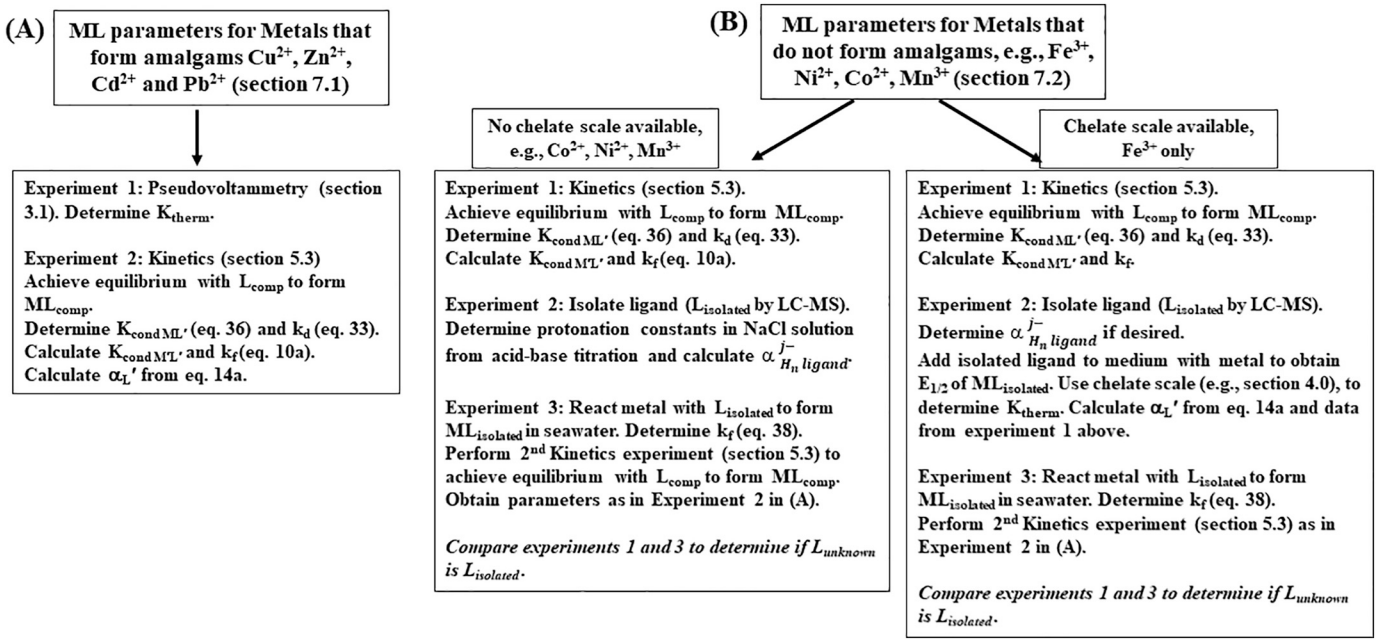

Appendix Fig. 12. Flow chart highlighting the protocol text in sections 7.1 and 7.2. Note that kinetics experiment 2 in pseudovoltammetry (A) is the same as experiments 1 and 3 in (B). $\alpha_{M'}$ in seawater is a known quantity.

References

Al-Farawati, R., van den Berg, C.M.G., 1999. Metal-sulfide complexation in seawater. Mar. Chem. 63, 331–352.

Baars, O., Croot, P.L., 2011. The speciation of dissolved zinc in the Atlantic sector of the Southern Ocean. Deep-Sea Res. II Top. Stud. Oceanogr. 58 (25–26), 2720–2732.

Bi, Z., Salaün, P., van den Berg, C.M.G., 2013. The speciation of lead in seawater by pseudo-polar graffiti using a silver amalgam micro wire electrode. Mar. Chem. 151, 1–12.

Boiteau, R.P., Till, C.P., Coale, T.H., Fitzsimmons, J.N., Bruland, K.W., Repeta, D.J., 2019. Patterns of iron and siderophore distributions across the California Current System. Limnol. Oceanogr. 64, 376–389.

Branica, G., Lovrić, M., 1997. Pseudopolarography of totally irreversible redox reactions. Electrochim. Acta 42, 1247–1251.

Bruland, K.W., 1989. Complexation of zinc by natural organic ligands in the central North Pacific. Limnol. Oceanogr. 34, 176–198.

Bruland, K.W., 1992. Complexation of cadmium by natural organic ligands in the central North Pacific. Limnol. Oceanogr. 37, 1008–1017.

Buck, K.N., Moffett, J., Barbeau, K.A., Bundy, R.A., Kondo, Y., Wu, J., 2012. The organic complexation of iron and copper: an intercomparison of competitive ligand exchange–adsorptive cathodic stripping voltammetry (CLE-ACSV) techniques. Limnol. Oceanogr. Methods 10, 496–515.

Buck, K.N., Lohan, M.C., Sander, S.G., Hassler, C., Pižeta, I., 2016. Editorial: organic ligands—a key control on trace metal biogeochemistry in the ocean. Front. Mar. Sci. 4, 313. https://doi.org/10.3389/fmars.2017.00313.

Bundy, R.M., Boiteau, R.M., McLean, C., Turk-Kubo, K.A., McIlvin, M.R., Saito, M.A., Van Mooy, S., Repeta, D.J., 2018. Distinct siderophores contribute to iron cycling in the mesopelagic at station ALOHA. Front. Mar. Sci. 5, 61. https://doi.org/10.3389/fmars.2018.00061.

Byrne, R.H., Kump, L.R., Cantrell, K.J., 1988. The influence of temperature and pH on trace metal speciation in seawater. Mar. Chem. 25, 163–181.

Capodaglio, G., Coale, K.H., Bruland, K.W., 1990. Lead speciation in surface waters of the eastern North Pacific. Mar. Chem. 29, 221–233.

Coale, K.H., Bruland, K.W., 1988. Copper complexation in the north East Pacific. Limnol. Oceanogr. 33, 1084–1101.

Croot, P.L., Heller, M.I., 2012. The importance of kinetics and redox in the biogeochemical cycling of iron in the surface ocean. Front. Microbiol. 3, 219. https://doi.org/10.3389/fmicb.2012.00219.

Croot, P.L., Heller, M.I., Schlosser, C., Wuttig, K., 2011. Utilizing radio-isotopes for trace metal speciation measurements in seawater. In: Singh, N (Ed.), Radioisotopes/ Book 1. In Tech, pp. 247–278.

Croot, P.L., Johansson, M., 2000. Determination of iron speciation by cathodic stripping voltammetry in seawater using the competing ligand 2-(2-Thiazolylazo)-p-cresol (TAC). Electroanalysis 12, 565–576.

Croot, P.L., Moffett, J.W., Luther III, G.W., 1999. Polarographic determination of half-wave potentials for copper-organic complexes in seawater. Mar. Chem. 67, 219–232. https://doi.org/10.1016/S0304-4203(99)00054-7.

Croot, P.L., Moffett, J.W., Brand, L.E., 2000. Production of extracellular cu complexing ligands by eucaryotic phytoplankton in response to Cu stress. Limnol. Oceanogr. 45, 619–627.

DeFord, D., Hume, D., 1951. The determination of consecutive formation constants of complex ions from polarographic data. J. Am. Chem. Soc. 73, 5321–5322.

Donat, J.R., Bruland, K.W., 1990. A comparison of two voltammetric techniques for determining zinc speciation in Northeast Pacific Ocean waters. Mar. Chem. 28, 301–323.

Erickson, H.P., 2009. Size and shape of protein molecules at the nanometer level determined by sedimentation, gel filtration, and electron microscopy. Biol. Proc. Online 11, 32–51. https://doi.org/10.1007/s12575-009-9008-x.

Fitzsimmons, J.N., Boyle, E.A., 2014. Assessment and comparison of Anopore and crossflow filtration for the determination of dissolved iron size fractionation into soluble and colloidal phases in seawater. Limnol. Oceanogr. Methods 12, 246–263.

Fitzsimmons, J.N., Boyle, E.A., Jenkins, W.J., 2014. Distal transport of dissolved hydrothermal iron in the deep South Pacific Ocean. Proc. Natl. Acad. Sci. U. S. A. 111, 16554–16661.

Gerringa, L.J.A., Rijkenberg, M.J.A., Wolterbeek, H.T., Verburg, T.G., Boye, M., Baar, H. J.W.D., 2007. Kinetic study reveals weak Fe-binding ligand, which affects the solubility of Fe in the Scheldt estuary. Mar. Chem. 103, 30–45.

Gerringa, L.J.A., Rijkenberg, M.J.A., Bown, J., Margolin, A.R., Laan, P., de Baar, H.J.W., 2016. Fe-binding dissolved organic ligands in the Oxic and Suboxic waters of the Black Sea. Front. Mar. Sci. 3, 84. https://doi.org/10.3389/fmars.2016.00084.

Gibbon-Walsh, K., Salaün, P., van den Berg, C.M.G., 2012. Pseudopolarography of copper complexes in seawater using a vibrating gold micro wire electrode. J. Phys. Chem. A 116, 6609–6620.

González, A.G., Cadena-Aizaga, M.I., Sarthou, G., González-Dávila, M., Santana-Casiano, J.M., 2019. Iron complexation by phenolic ligands in seawater. Chem. Geol. 511, 380–388.

Hassler, C.S., van den Berg, C.M.G., Boyd, P.W., 2016. Toward a regional classification to provide a more inclusive examination of the ocean biogeochemistry of Iron-binding ligands. Front. Mar. Sci. 4, 19. https://doi.org/10.3389/fmars.2017.00019.

Hochella, M.F., Mogk, D.W., Ranville, J., Allen, I.C., Luther, G.W., Marr, L.C., McGrail, B. P., Murayama, M., Qafoku, N.P., Rosso, K.M., Sahai, N., Schroeder, P.A., Vikesland, P., Westerhoff, P., Yang, Y., 2019. Natural, incidental, and engineered nanomaterials and their impacts on earth systems. Science 363, 1414. https://doi.org/10.1126/science.aau8299.

Holt, P.D., Reid, R.R., Lewis, B., Luther III, G.W., Butler, A., 2005. Fe(III)coordination chemistry of Alterobactin A: a Siderophore from the marine bacterium Alteromonas luteoviolacea. Inorg. Chem. 44, 7671–7677.

Hudson, R.J.M., Covault, D.T., Morel, F.M.M., 1992. Investigation of iron coordination and redox reactions in seawater using ^{59}Fe radiometry and ion-pair solvent extraction of amphilic iron complexes. Mar. Chem. 38, 209–235.

Kim, J.-M., Baars, O., Morel, F.M.M., 2015. Bioavailability and electroreactivity of zinc complexed to strong and weak organic ligands. Environ. Sci. Technol. 49, 10894–10902. https://doi.org/10.1021/acs.est.5b02098.

Kim, J.-M., Baars, O., Morel, F.M.M., 2016. The effect of acidification on the bioavailability and electrochemical lability of zinc in seawater. Philos. Trans. R. Soc. A Math. Phys. Eng. Sci. 374 (2081) https://doi.org/10.1098/rsta.2015.0296.

Laglera, L.M., van den Berg, C.M.G., 2009. Evidence for geochemical control of iron by humic substances in seawater. Limnol. Oceanogr. 54, 610–619.

Langford, C.H., Gray, H.B., 1965. Ligand Substitution Processes. W.A. Benjamin, New York.

Lewis, B.L., Luther III, G.W., Lane, H., Church, T.M., 1995a. Determination of metal-organic complexation in natural waters by SWASV with pseudopolarograms. Electroanalysis 7, 166–177. https://doi.org/10.1002/elan.1140070213.

Lewis, B.L., Holt, P.D., Taylor, S.W., Wilhelm, S.W., Trick, C.G., Butler, A., Luther III, G. W., 1995b. Voltammetric estimation of iron(III) thermodynamic stability constants for catecholate siderophores isolated from marine bacteria and cyanobacteria. Mar. Chem. 50, 179–188. https://doi.org/10.1016/0304-4203(95)00034-O.

Loomis, L.D., Raymond, K.N., 1991. Solution equilibria of enterobactin and metal-enterobactin complexes. Inorg. Chem. 30, 906–911.

Lovrić, M., 1998. A simulation of an initial stage of a Pseudopolarographic experiment on a thin mercury film covered rotating disk electrode. Electroanalysis 10, 1022–1025.

Luther, G.W., 2016. Inorganic Chemistry for Geochemistry and Environmental Sciences: Fundamentals and Applications. John Wiley & Sons Ltd. https://doi.org/10.1002/9781118851432

Luther III, G.W., Theberge, S.M., Rickard, D.T., 1999. Evidence for aqueous clusters as intermediates during zinc sulfide formation. Geochim. Cosmochim. Acta 63, 3159–3169. https://doi.org/10.1016/S0016-7037(99)00243-4.

Luther III, G.W., Theberge, S.M., Rickard, D., 2000. Determination of stability constants for metal-ligand complexes using the voltammetric oxidation wave of the anion/ligand and the DeFord and Hume formalism. Talanta 51, 11–20. https://doi.org/10.1016/S0039-9140(99)00234-9.

Luther III, G.W., Madison, A.S., Mucci, A., Sundby, B., Oldham, V.E., 2015. A kinetic approach to assess the strengths of ligands bound to soluble Mn(III). Mar. Chem. 173, 93–99. https://doi.org/10.1016/j.marchem.2014.09.006.

Madison, A.S., Tebo, B.M., Luther III, G.W., 2011. Simultaneous determination of soluble manganese(III), manganese(II) and total manganese in natural (pore)waters. Talanta 84, 374–381. https://doi.org/10.1016/j.talanta.2011.01.025.

Maldonado, M.T., Price, N.M., 2001. Reduction and transport of organically bound iron by Thalassiosira oceanica (Bacillariophyceae). J. Phycol. 37, 298–309. https://doi.org/10.1046/j.1529-8817.2001.037002298.x.

Martell, A.E., Smith, R.M., 1974. Critical Stability Constants, 1: Amino Acids. Plenum Press, New York and London.

Martell, A.E., Smith, R.M., 1977. Critical Stability Constants, 3: Other Organic Ligands. Plenum Press, New York and London.

Martell, A.E., Smith, R.M., 1982. Critical Stability Constants, 5: First Supplement. Plenum Press, New York and London.

Martell, A.E., Smith, R.M., 1986. Critical Stability Constants, 6. Plenum Press, New York and London.

Nicolau, R., Louis, Y., Omanović, D., Garnier, C., Mounier, S., Pižeta, I., 2008. Study of interactions of concentrated marine dissolved organic matter with copper and zinc by pseudopolarography. Anal. Chim. Acta 618, 35–42.

Omanović, D., Branica, M., 2004. Pseudopolarography of trace metals. Part II. The comparison of the reversible, quasireversible and irreversible electrode reactions. J. Electroanal. Chem. 565 (1), 37–48.

Omanović, D., Garnier, C., Pižeta, I., 2015. ProMCC: an all-in-one tool for trace metal complexation studies. Mar. Chem. 173, 25–39.

Pađan, J., Marcinek, S., Cindrić, A.-M., Santinelli, C., Brogi, W.R., Radakovitch, O., Garnier, C., Omanović, D., 2021. Organic copper speciation by anodic stripping voltammetry in estuarine waters with high dissolved organic matter. Front. Chem. 8 (1306) https://doi.org/10.3389/fchem.2020.628749.

Pearson, R.G., 1988. Absolute electronegativity and hardness: application to inorganic chemistry. Inorg. Chem. 27, 734–740.

Pižeta, I., Sander, S.G., Hudson, R.J.M., Omanović, D., Baars, O., Barbeau, K.A., Buck, K. N., Bundy, R.M., Carrasco, G., Croot, P.L., Garnier, C., Gerringa, L.J.A., Gledhill, M., Hirose, K., Kondoo, Y., Laglera, L.M., Nuester, J., Rijenberg, M.J.A., Takeda, S., Twining, B.S., Wells, M., 2015. Interpretation of complexometric titration data: an intercomparison of methods for estimating models of trace metal complexation by natural organic ligands. Mar. Chem. 173, 3–24.

Purawatt, S, Siripinyanond, A, Shiowatana, J, 2007. Flow field–flow fractionation–inductively coupled optical emission spectrometric investigation of the size-based distribution of iron complexed to phytic and tannic acids in a food suspension: implications for iron availability. Anal. Bioanal. Chem. 389, 733–742. https://doi.org/10.1007/s00216-007-1308-x.

Reid, R.T., Live, D.H., Faulkner, D.J., Butler, A., 1993. A siderophore from a marine bacterium with an exceptional ferric ion stability constant. Nature 366, 455–458.

Ringbom, A., Still, E., 1972. The calculation and use of α coefficients. Anal. Chim. Acta 59, 143–146.

Rose, A.L., Waite, T.D., 2003a. Kinetics of hydrolysis and precipitation of ferric iron in seawater. Environ. Sci. Technol. 37, 3897–3903.

Rose, A.L., Waite, T.D., 2003b. Kinetics of iron complexation by dissolved natural organic matter in coastal waters. Mar. Chem. 84, 85–103.
Rozan, T.F., Luther III, G.W., Ridge, D., Robinson, S., 2003. Determination of Pb complexation in oxic and sulfidic waters using Pseudovoltammetry. Environ. Sci. Technol. 37, 3845–3852. https://doi.org/10.1021/es034014r.
Rue, E.L., Bruland, K.W., 1995. Complexation of iron(III) by natural organic ligands in the central North Pacific as determined by a new competitive ligand equilibration adsorptive cathodic stripping voltammetric method. Mar. Chem. 50, 117–138.
Saňudo-Wilhelmy, S.A., Rivera-Duarte, I., Flegal, A.R., 1996. Distribution of colloidal trace metals in the San Francisco Bay estuary. Geochim. Cosmochim. Acta 60, 4933–4944.
Schijf, J., Burns, S.M., 2016. Determination of the side reaction coefficient of Desferrioxamine B in trave metal clean seawater. Front. Mar. Sci. 3, 117. https://doi.org/10.3389/fmars.2016.00117.
Schlosser, C., Croot, P.L., 2008. Application of cross-flow filtration for determining the solubility of iron species in open ocean seawater. Limnol. Oceanogr. Methods 6, 630–642. https://doi.org/10.4319/lom.2008.6.630.
Spasojević, I., Armstrong, S.K., Brickman, T.J., Crumbliss, A.L., 1999. Electrochemical behavior of the Fe(III) complexes of the cyclic hydroxamate siderophores alcaligin and desferrioxamine E. Inorg. Chem. 38, 449–454.
Taylor, S.W., Luther III, G.W., Waite, J.H., 1994. Polarographic and spectrophotometric investigation of iron(III) complexation to 3,4-dihydroxyphenylalanine-containing peptides and proteins from *Mytilus edulis*. Inorg. Chem. 33, 5819–5824. https://doi.org/10.1021/ic00103a032.
Thibault de Chanvalon, A., Luther III, G.W., 2019. Mn speciation at nanomolar concentrations with a porphyrin competitive ligand and UV-vis measurements. Talanta 200, 15–21. https://doi.org/10.1016/j.talanta.2019.02.069.
Tsang, J.T., Rozan, T.F., Hsu-Kim, H., Mullaugh, K.M., Luther III, G.W., 2006. Pseudopolarographic determination of Cd^{2+} complexation in freshwater. Environ. Sci. Technol. 40, 5395–5401. https://doi.org/10.1021/es0525509.
van den Berg, C.M.G., 1995. Evidence for organic complexation of iron in seawater. Mar. Chem. 50, 139–157.
van den Berg, C.M.G., 2006. Chemical speciation of iron in seawater by cathodic stripping voltammetry with dihydroxynaphthalene. Anal. Chem. 78, 156–163.
Waterbury, R.D., Yao, W., Byrne, R.H., 1997. Long pathlength absorbance spectroscopy: trace analysis of Fe(II) using a 4.5 m liquid core waveguide. Anal. Chim. Acta 357, 99–102.
Witter, A.E., Luther III, G.W., 1998. Variation in Fe(III)-organic complexation with depth in the northwestern Atlantic Ocean as determined using a kinetic approach. Mar. Chem. 62, 241–258. https://doi.org/10.1016/S0304-4203(98)00044-9.
Witter, A.E., Hutchins, D.A., Butler, A., Luther III, G.W., 2000. Determination of conditional stability constants and kinetic constants for strong Fe-binding ligands in seawater. Mar. Chem. 69, 1–17. https://doi.org/10.1016/S0304-4203(99)00087-0.
Wu, J., Luther III, G.W., 1995. Complexation of iron(III) by natural organic ligands in the Northwest Atlantic Ocean by a competitive ligand equilibration method and a kinetic approach. Mar. Chem. 50, 159–177. https://doi.org/10.1016/0304-4203(95)00033-N.
Wuttig, K., Heller, M.I., Croot, P.L., 2013. Reactivity of inorganic Mn and Mn desferrioxamine B with O_2, O^{-2}, and H_2O_2 in seawater. Environ. Sci. Technol. 47, 10257–10265. https://doi.org/10.1021/es4016603.
Yücel, M., Gartman, A., Chan, C.S., Luther III, G.W., 2011. Hydrothermal vents as a kinetically stable source of iron-sulphide-bearing nanoparticles to the ocean. Nat. Geosci. 4, 367–371. https://doi.org/10.1038/NGEO1148.
Zeng, H., Hwang, D.S., Israelachvili, J.N., Waite, J.H., 2010. Strong reversible Fe3+−mediated bridging between Dopa containing protein films in water. Proc. Natl. Acad. Sci. U. S. A. 107, 12850–12853.